TASK R

Quarterly Progress Report No.10
for the period
1 July-30 September 1961

TASK R IS A PROGRAM OF RESEARCH IN BASIC PHENOMENA
ASSOCIATED WITH THE BEHAVIOR OF MATERIALS IN HIGH
TEMPERATURE GAS ENVIRONMENTS. IT IS SUPPORTED BY
THE ADVANCED RESEARCH PROJECTS AGENCY THROUGH
CONTRACT NORD 7386 WITH THE BUREAU OF NAVAL WEAPONS,
DEPARTMENT OF THE NAVY.

THE JOHNS HOPKINS UNIVERSITY
APPLIED PHYSICS LABORATORY
8621 GEORGIA AVENUE   SILVER SPRING, MARYLAND

TASK R

Quarterly Progress Report No.10
for the period
1 July-30 September 1961

GENERAL OBJECTIVES OF TASK R

Many of the wide variety of problems associated with the use of materials at high temperatures occur in connection with advanced propulsion systems, and of these, some of the most critical and complex are encountered in high performance rocket motors. Present trends in rocket design and propellant formulation resulting in gas flows of increased temperature, pressure, and corrosiveness may be expected to aggravate the materials situation. It seems self-evident that future, long-range solutions to these problems must rely on more sophisticated approaches and broader knowledge of the behavior of materials in high temperature gas environments than is characteristic of the usual "quick-fix", or expensive cut-and-try test procedures. It also seems likely that improvement in structural materials themselves (i.e., higher strength at high temperature, higher melting point, etc.) has reached the point of diminishing returns, so that various other subterfuges must be tried.

Research performed under Task R at the Applied Physics Laboratory or its subcontracting agencies is intended to provide some of the fundamental knowledge necessary for a rational understanding of the behavior of materials at high temperatures. This is a very broad and very complex field involving many different scientific disciplines. While no attempt is made to rigidly limit the scope of Task R, the general emphasis is on appropriate research in the flow and physical chemistry of high temperature gases such as are characteristic of advanced solid propellant rocket motors, and the phenomena basic to heat transfer and cooling techniques in such environments, rather than in the properties of materials themselves.

A. A. Westenberg
Program Coordinator

SUMMARY

The scavenger probe sampling technique was tried on a CH_4-O_2 flame using NO_2 to scavenge for O-atoms. Results very close to the calculated thermodynamic equilibrium value in the burned gas region were obtained, and a qualitatively reasonable non-equilibrium maximum was measured in the reaction zone.

Final results of measurements by the new line source technique on N_2, CO_2, and N_2-CO_2 mixtures over the temperature range 300-1100°K are presented and compared with kinetic theory calculations. Apparatus changes required for study of the H_2O-O_2 system are described.

Boundary layer temperature profile data are reported for the Mach 4.5 station in the nozzle. These are shown to bear out closely the Reynolds analogy between heat transfer and skin friction. Some heat transfer results on a cooled copper nozzle are given. Efforts to overcome noise problems in the infrared spectroscopic equipment are described, and a discussion is given of two new radiation pyrometers developed for measuring nozzle surface temperatures.

Numerical solutions to the flow of a real propellant gas with complex kinetic kinetics are presented. The exact solution is compared with several approximate solutions to point out the relative importance of different elementary reaction steps.

I. HIGH TEMPERATURE CHEMICAL KINETICS IN LAMINAR FLAMES

(R. M. Fristrom, C. Grunfelder, A. A. Westenberg)

Objective

The effect of chemical reactions is one of the important problems
in the dynamics of high temperature, high speed gas flow. Chemistry and
aerodynamics (and sometimes molecular transport processes) are strongly
coupled in various nozzle flow and boundary layer phenomena. Advances in
understanding in these areas cannot be made without a great deal more
knowledge of high temperature chemical kinetics than is presently available.
The important reactions are extremely rapid and lie in temperature regions
where materials present problems. Therefore, conventional experimental
techniques are not generally applicable, and the extrapolation of infor-
mation from lower temperature reaction rate studies is not satisfactory.
The approach taken in this project is to study high temperature kinetics
by a detailed quantitative analysis of laminar flame structure. From this
analysis it is hoped that eventually the kinetics of elementary combustion
reactions can be obtained. The present work allows the determination of
the rates of appearance or disappearance of all of the stable species in
a flame as a function of position (or time), temperature, and chemical
composition. This is the same type of data obtained in conventional
kinetic studies, and a much wider temperature range is accessible.

The main problem in the derivation of chemical kinetic constants
from flame structure data is the lack of information on the concentrations
of radical and atom species. This problem is not unique to flame studies,

but in conventional chemical kinetic studies the steady-state approximation is used to circumvent the difficulty. Flame chemistry is often too complex for this method and there is considerable doubt as to the validity of the approximations in many flame systems. Therefore, we consider this to be an experimental problem. We have undertaken development of a technique to provide this information. The so-called scavenger probe method combines the techniques of probe sampling with those of chemical scavenging. The principle is straightforward: A sample of the radical-containing gas is withdrawn rapidly so that the composition of the gas is effectively frozen. This can be accomplished by using a properly designed nozzle and a fast pump. These radical-containing gases are then mixed with an excess of a scavenger species which reacts quantitatively with the radical to give a characteristic product.

Scavenger Experiments

During preceding quarters an apparatus employing a chlorinated hydrocarbon oil as a scavenger for H-atoms was described (Ref. 1). The system gave reproducible and qualitatively reasonable profiles of H-atom concentration, but after extensive comparisons with the values calculated for thermodynamic equilibrium in the burned gas region of several flames, it was concluded that the efficiency of scavenging was unsatisfactory. A reconsideration of the rates involved indicated that the wall recombination was too high and that the oil film on the walls did not prevent this as originally hoped.

It appeared that an even faster scavenger reaction and/or lower wall recombination rates would be required. This would mean a scavenger activation energy lower than 5 kcal/mole or a wall recombination coefficient

below 10^{-4}. Since the reaction of O with NO_2 is reportedly one of the fastest bimolecular reactions known, work was measured on O-atoms using NO_2 as scavenger according to $O + NO_2 \longrightarrow NO + O_2$. The reason for suspending work on this originally was the difficulty in separating out the NO_2 and the bad behavior of the latter in the mass spectrometer (Ref. 2). The cracking pattern for NO_2 (i.e., the peak ratio 30/46) showed periodic variations which made quantitative work difficult since this interfered with NO detection on the 30 peak. This trouble with NO_2 has been noted by others and is probably due to reaction on the hot filament to form varying amounts of NO depending on pump fluctuations.

A water-cooled probe system using a 3-liter reaction flask was set up, and by arranging to determine the 30/46 rates (with no O-atoms present) immediately before each run it was possible to obtain results indicating that sampling and scavenging were close to 100% effective. Referring to Fig. I-1, a profile of O-atom concentration determined in this way shows very close to the calculated value of 0.2 mole per cent in the burned gas region, and a non-equilibrium maximum in the reaction zone of the flame which is qualitatively as expected.

Even these results are not considered satisfactory because of irreproducibility, probably due to the long pump out time required. Since it appeared that the 3-liter volume was not necessary for the scavenging reaction and was detrimental otherwise, the system was redesigned for minimum volume and faster pumping. In addition, provision was made for inserting a silver "spoiler" to make certain that all O-atoms were recombined before reaching the NO_2 bypass injection point used to
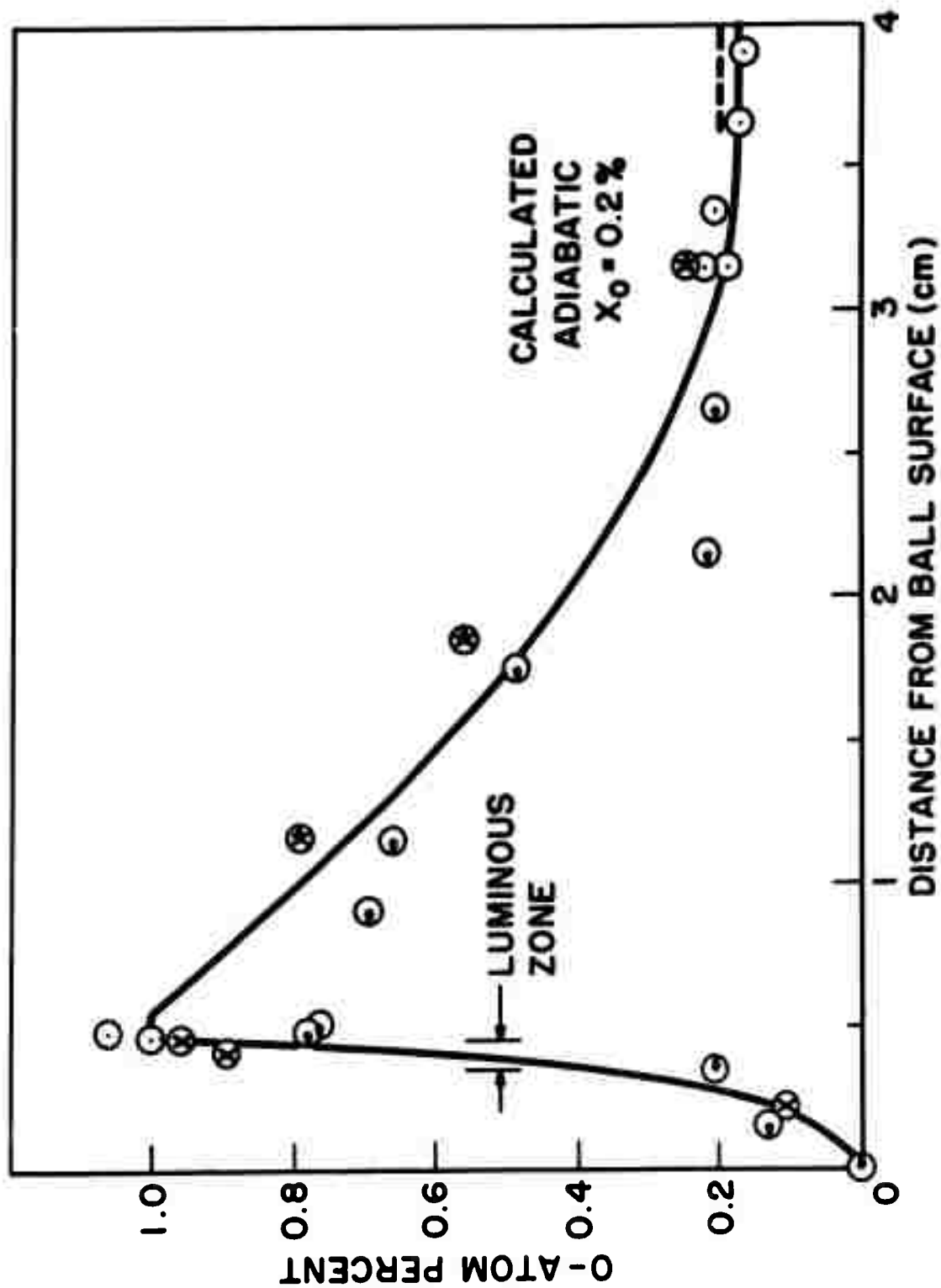
Fig. I-1 O-ATOM PROFILE IN A SPHERICAL FLAME (CH_4 + 2.2 O_2 + 8.8 Ar) DETERMINED BY SCAVENGING WITH NO_2

Pressure = 4.1 cm Hg. The variously labeled points represent results from different runs.

determine the blank 30/46 ratio. This new system and procedure proved to be more convenient and reproducible, but the absolute values in the burned gas region were again too low. Careful examination of the probe showed luminous spots in the critical uncooled region near the probe tip which were due to atom recombination on tiny particles of glass remaining from the construction process. This difficulty reappeared even after cleaning, so it was evident that the system should be arranged with the probe inverted so that its tip would be on top instead of the lowest point in the system as at present. This should prevent dirt and other unwanted particles from falling into the probe tip region. Such a rearrangement is presently being carried out.

References

1) Task R Quarterly Progress Report No. 8, APL/JHU Report TG 331-8.

2) Task R Quarterly Progress Report No. 5, APL/JHU Report TG 331-5.

II. THERMAL CONDUCTIVITY OF GASES

(N. deHaas and A. A. Westenberg)

Objective

The analysis of the problem of convective heat transfer both in the laminar and turbulent flow regimes requires that the properties of the gases involved be quantitatively understood. The coefficient of thermal conductivity is one such property. Measurement of thermal conductivity of gases has not been a forsaken field of research, and several common gases have been investigated up to temperatures approaching reaction motor temperatures. The primary shortcomings of past and present research in the study of thermal conductivity of gases for application to such heat transfer problems are: a) Inability to apply present experimental methods to temperatures above about 1000°K (most measurements are made at substantially lower temperatures than this), b) the complexity and difficulty in using the usual apparatus for this measurement (thermal-conductivity cells), and 3) the lack of measurements of species (and mixtures) prevalent in reaction motors. Other shortcomings could be listed.

Recent measurements of molecular diffusion coefficients - a closely related transport property - of common flame gases at temperatures in excess of 1000°K applied a simple concept that could, in principle, be used for measuring other gas transport properties (conductivity and viscosity). In this method, a point source of a trace gas is located in the center of a uniform, heated laminar jet of a second gas. A series of gas samples removed immediately downstream of the source and quantitatively analyzed is used to determine the molecular diffusion coefficient. The technique has good precision (±1-2%) and is quite adaptable to high temperatures and various gas types.

Adaptation of this method to the measurement of thermal conductivity of gases is an obvious extension. The source of trace gas is replaced with a line source of heat and the temperature rise downstream of the heat source is measured with an appropriate technique. The method is simple, has good precision, and can be used with a variety of pure gases and gas mixtures at high ambient temperature (approaching flame temperatures). The objective of this research is to use this method of measuring the thermal conductivities of gases to obtain data over a wide range of temperature on pure gases and mixtures of propulsion interest.

Summary of Progress To Date

The line source method for the measurement of gas thermal conductivity at high temperatures has been developed to the point where the precision of measurement is about $\pm 2\%$. The theory, experimental technique, and apparatus for this method have been given in previous reports in this series and a publication of preliminary results for N_2 and He at room temperature was made (Ref. 1).

During the period of this report the measurements on N_2, CO_2, and mixtures of the two gases in the range $300-1050°K$ were concluded. The results for those gases which were not previously reported (Ref. 2) are presented in the next section. A paper entitled "High Temperature Gas Diffusivity Measurement with the Line Source Technique" has been accepted for presentation at the Second Symposium on Thermophysical Properties. A paper presenting the results of N_2, CO_2, and their mixtures is being prepared for publication in the Physics of Fluids. The apparatus is now being readied for measurements of H_2O-O_2 mixtures.

Final Results for N_2, CO_2 and Their Mixtures

The final results for these gases are presented in Figs. II-1, II-2, II-3, II-4, II-5, and II-6 as well as in Table II-1. Included in the graphs of thermal conductivity vs. temperature for the two pure gases and the three mixtures are the results of other investigators which we regard as most reliable. The agreement is quite good although there is considerable scatter in our results at the highest temperatures in the case of CO_2, .75 CO_2 and .25 CO_2. The cause of this excessive scatter is not known, but it is believed that it can be improved. The smoothed curves in the figures were drawn through all the plotted data and represent the best fit to the data present available.

Table II-1. Thermal conductivities of N_2, CO_2 and N_2-CO_2 Mixtures. Smoothed values taken from curves of Figs. II-1 through II-5.

λ (cal cm^{-1} sec^{-1} °K^{-1} x 10^5)

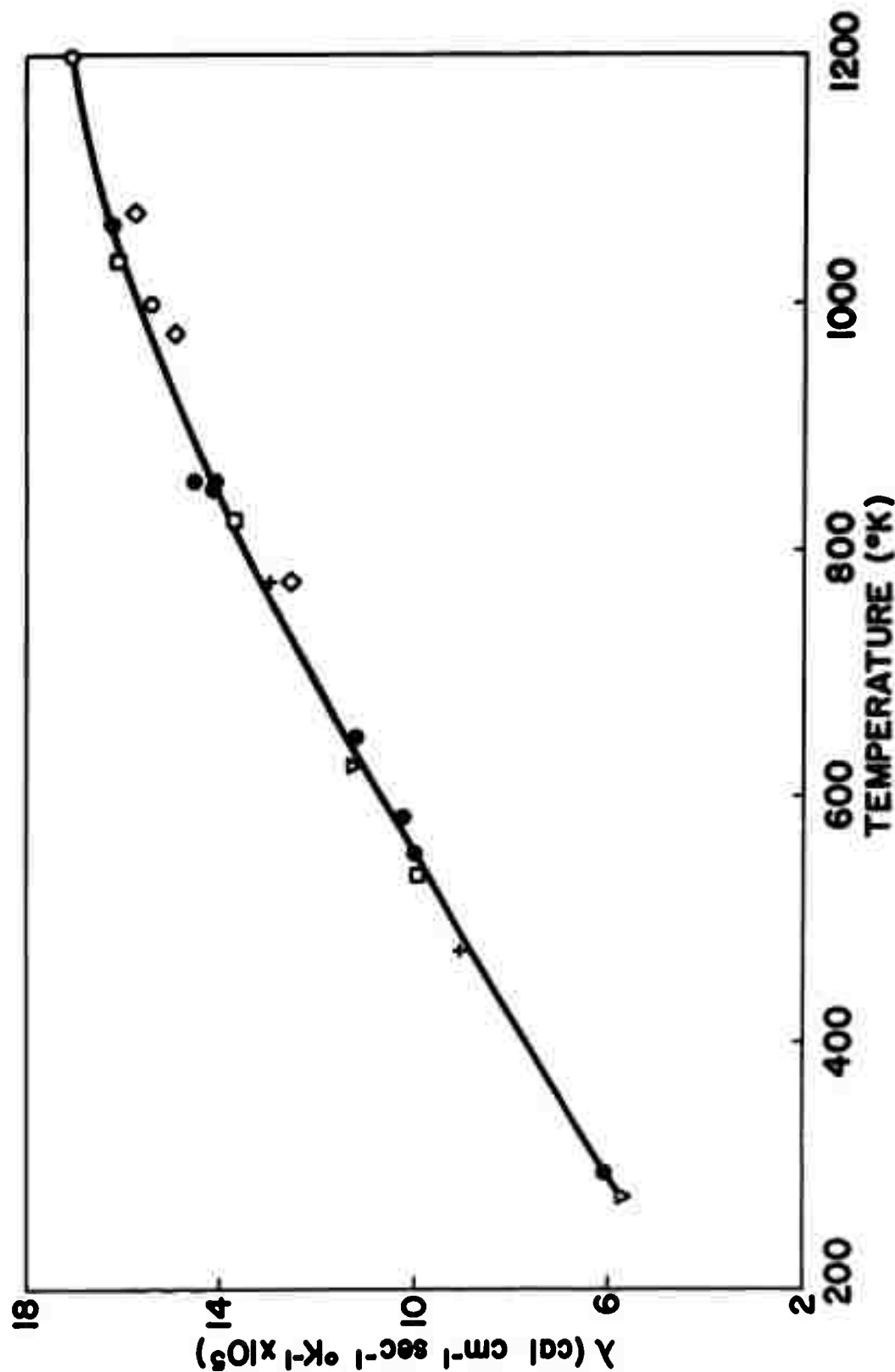| Temperature (°K)	N_2	25% CO_2	50% CO_2	75% CO_2	CO_2
300	6.13	5.25	4.85	4.30	3.93
400	7.65	7.1	6.80	6.2	5.90
500	9.15	8.9	8.75	8.2	7.8
600	10.7	10.7	10.6	10.0	9.8
700	12.1	12.3	12.5	11.8	11.7
800	13.5	13.8	14.2	13.4	13.5
900	14.7	15.2	15.8	14.9	15.3
1000	15.7	16.4	17.1	16.3	16.8
1100	16.5	-	18.0	-	17.9

Fig. II-1 COMPARISON OF MEASUREMENTS OF THERMAL CONDUCTIVITY OF
OF NITROGEN WITH VALUES REPORTED IN THE LITERATURE

● this work (mean deviation from smooth curve: 1.4%);
▽ Keyes (Ref. 4); + Nuttall and Ginnings (Ref. 5);
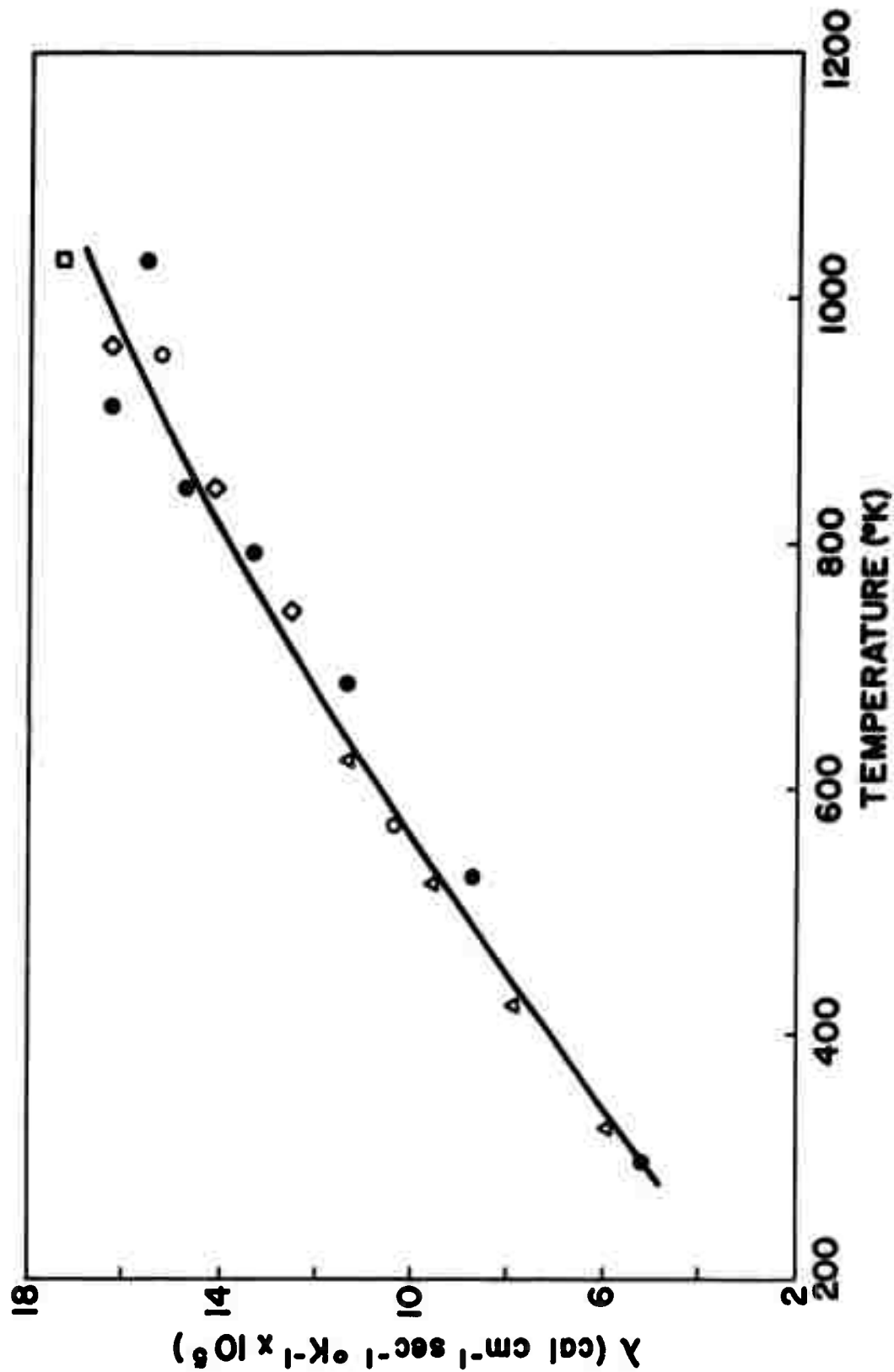◇ Rothman and Bromley (Ref. 6); ○ Stops (Ref. 7);
□ Vines (Ref. 8).

Fig. II-2 COMPARISON OF MEASUREMENTS OF THERMAL CONDUCTIVITY OF
MIXTURES OF 75 MOLE PER CENT NITROGEN -- 25 MOLE
PER CENT CARBON DIOXIDE WITH VALUES REPORTED
IN THE LITERATURE

● this work (mean deviation from smooth curve: 3.4%);
▽ Keyes (Ref. 4); ◇ Rothman and Bromley (Ref. 6);
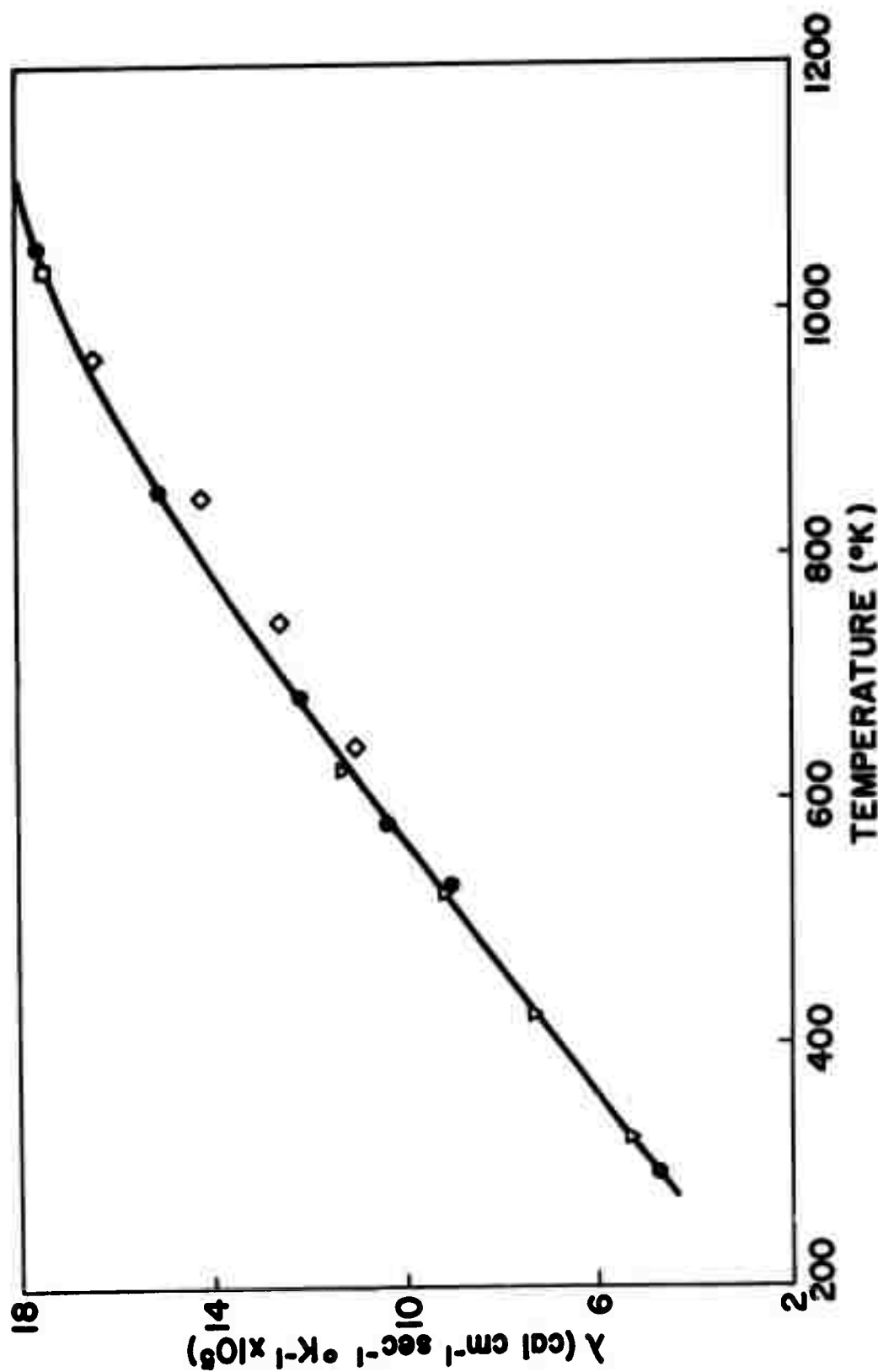□ Vines (Ref. 8).

Fig. II-3 COMPARISON OF MEASUREMENTS OF THERMAL CONDUCTIVITY OF
MIXTURES OF 50 MOLE PER CENT NITROGEN -- 50 MOLE PER CENT
CARBON DIOXIDE WITH VALUES REPORTED IN THE LITERATURE

● this work (mean deviation from smooth curve: 1.6%);
▽ Keyes (Ref. 4); ◇ Rothman and Bromley (Ref. 6);
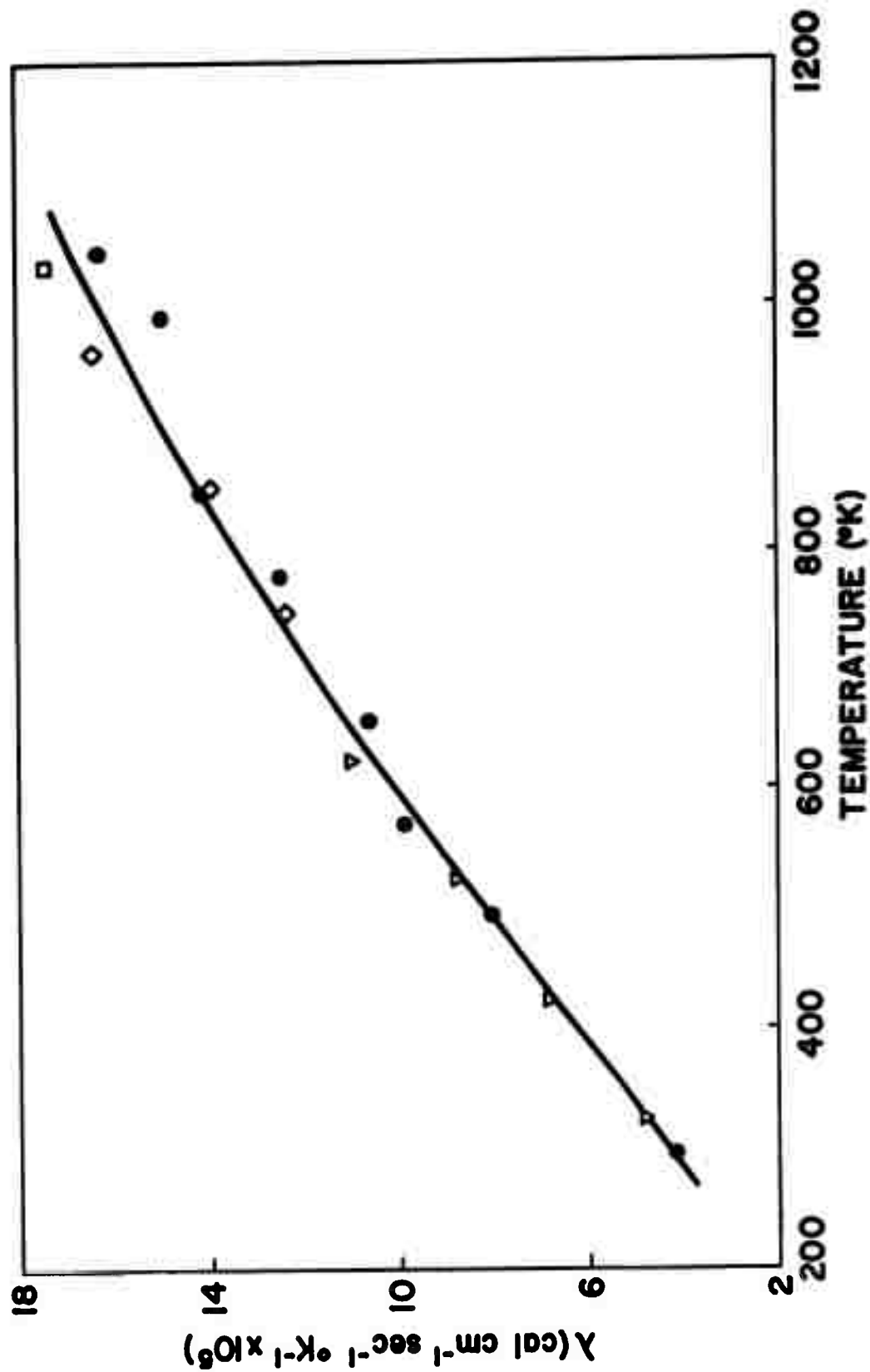□ Vines (Ref. 8).

Fig. II-4 COMPARISON OF MEASUREMENTS OF THERMAL CONDUCTIVITY OF
MIXTURES OF 25 MOLE PER CENT NITROGEN -- 75 MOLE PER CENT
CARBON DIOXIDE WITH VALUES REPORTED IN THE LITERATURE

● this work (mean deviation from smooth curve: 2.8%);
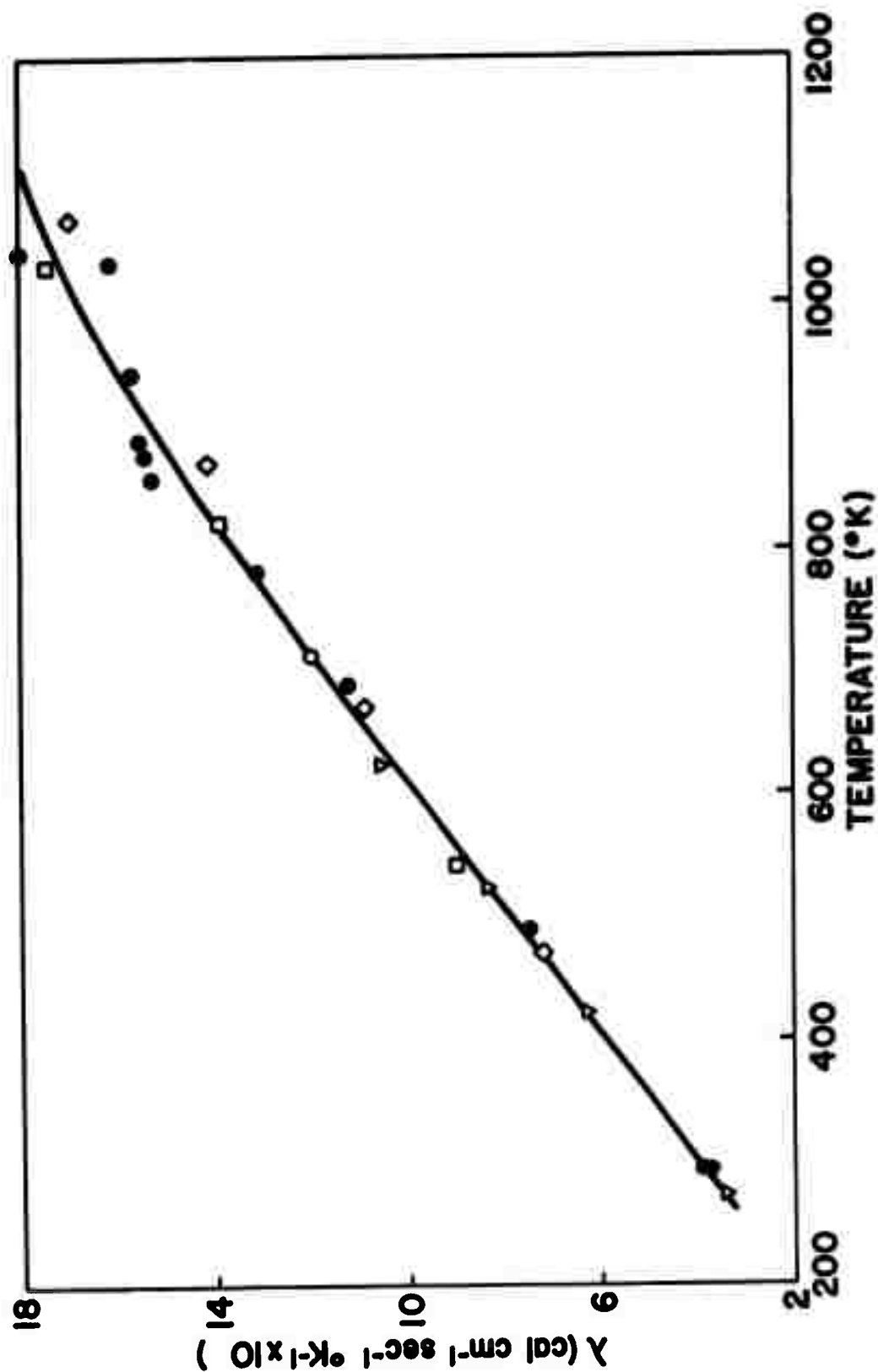▽ Keyes (Ref. 4); ◇ Rothman and Bromley (Ref. 6);
□ Vines (Ref. 8).

Fig. II-5 COMPARISON OF MEASUREMENTS OF THERMAL CONDUCTIVITY OF OF CARBON DIOXIDE WITH VALUES REPORTED IN THE LITERATURE

● this work (mean deviation from smooth curve: 2.2%);
▽ Keyes (Ref. 4);   ◇ Rothman and Bromley (Ref. 6);
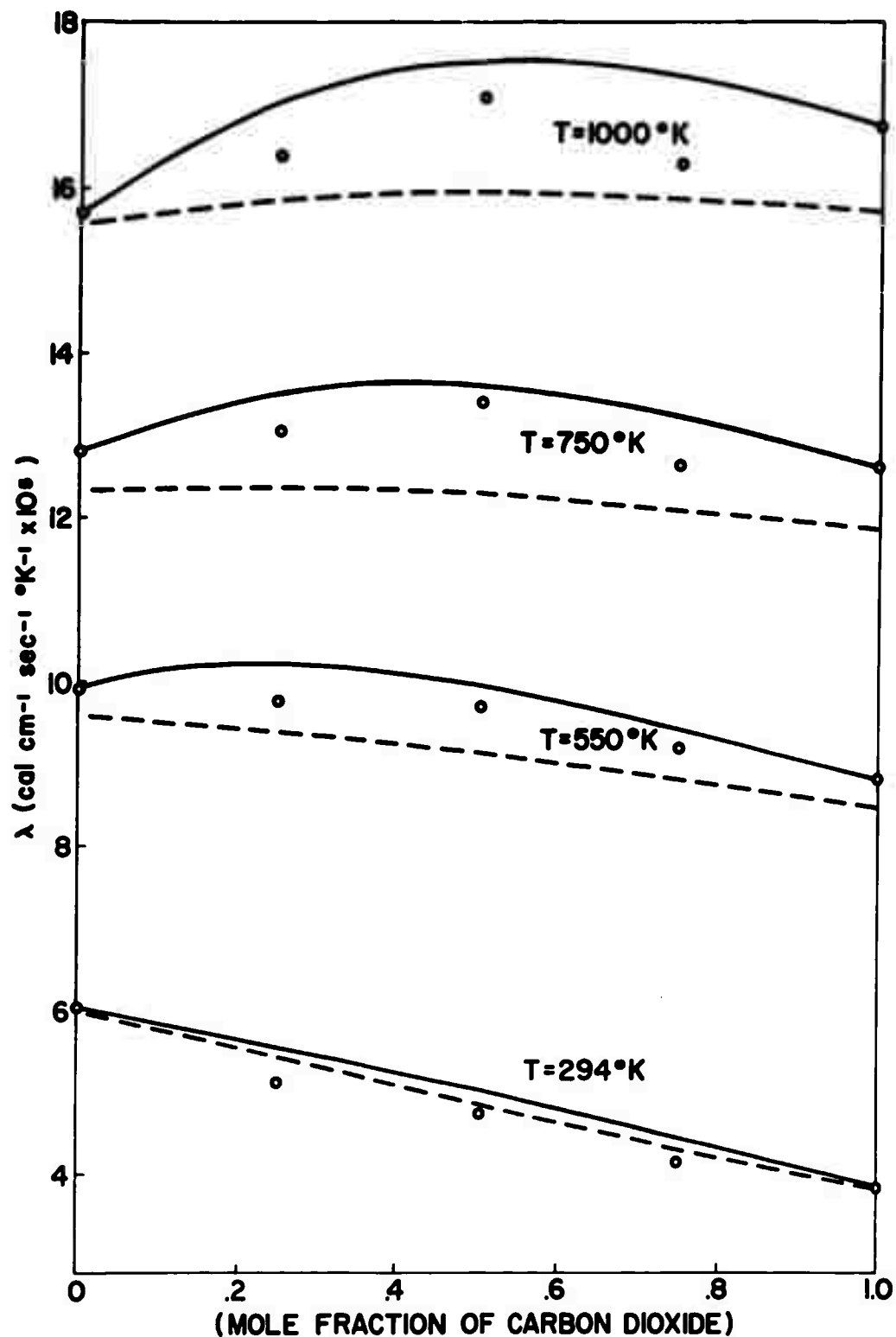○ Stops (Ref. 7);   □ Vines (Ref. 8).

Fig. II-6 COMPARISON OF THEORETICAL THERMAL CONDUCTIVITY OF MIXTURES
OF NITROGEN AND CARBON DIOXIDE WITH EXPERIMENTAL MEASUREMENTS

Indicated points taken from smoothed plots of measured λ versus T.
Solid line: Theoretical thermal conductivity obtained by "best"
method outlined in Ref. 2. Broken line: Theoretical thermal
conductivity obtained using viscosity force constants throughout.

Fig. II-6 gives a comparison of the theoretical thermal conductivity of mixtures of nitrogen and carbon dioxide with our experimental results. The solid lines were computed using a theoretical method previously outlined (Ref. 2). This computation made use of the best available experimental viscosity data for self-diffusion coefficients and frozen thermal conductivity of the pure gases, and experimental data on the binary diffusion coefficients and pure gas thermal conductivities. The broken lines in Fig. II-6 were computed as completely as possible from theory using a single set of viscosity-derived force constants. Thus λ_1^o, D_{11}, and D_{12} were obtained from the standard kinetic theory relations and force constants (Ref. 3), since this is the way one would be forced to do it in the usual case when experimental binary diffusion and pure gas thermal conductivities are not available. The computation of the latter made use of the most recent results on the Euchen correction (Ref. 9).

O_2, H_2O and Mixtures of O_2 and H_2O: Description of Apparatus

The later portion of the period of this report has been spent in adapting the apparatus for use in the measurement of the thermal conductivity of O_2, H_2O and their mixtures. Some rebuilding of the original apparatus was also required. The changes are in the gas flow system only (the means of producing a line source of heat, the thermocouple system for measuring the gas temperature rise, and the hot-wire arrangement for measuring the gas velocity have not been altered). A tracing of the gas flows will point out the alterations in the apparatus. Oxygen gas is

metered through a calibrated critical orifice and then passes into an "atomizing" chamber through a 0.06 in. hole. Liquid H_2O is metered through a calibrated orifice after which it passes into the atomizing chamber through the end of a drawn down (to 0.01 in.) quartz tube which is positioned at the 0.06 in. entrance hole of the atomizing chamber. The oxygen thus passes at sonic speed around the drawn quartz tip and acts to "atomize" the H_2O. The resulting mixture of O_2 and H_2O is heated from a surrounding 2 KW furnace to vaporize the H_2O. The gas mixture then flows into the usual main furnace where it is heated to the desired temperature. A water-cooled condenser is positioned at the jet exit to remove the water from the gas mixture.

Liquid water for the atomizer is supplied from a reservoir, which is pressurized by nitrogen gas. The pressure in this reservoir is regulated at a given level to provide a constant flow of water into the atomizing jet. The atomizer was patterned after that described by Calcote (Ref. 10). It is presently being built and checked out.

References

1. R. E. Walker, N. deHaas, and A. A. Westenberg, Phys. Fluids 3, 482 (1960).

2. Task R Quarterly Progress Report, The Johns Hopkins University, Applied Physics Laboratory Report No. TG-331-9.

3. J. O. Hirschfelder, C. F. Curtiss, and R. B. Bird, The Molecular Theory of Gases and Liquids, Wiley, New York (1954).

4. F. G. Keyes, Trans. ASME 74, 1303 (1952).

5. R. L. Nuttall and D. C. Ginnings, J. Res. Natl. Bur. Stds. 58, 271 (1957).

6. A. J. Rothman and L. A. Bromley, Ind. Eng. Chem. 47, 899 (1955).

7. D. W. Stops, Nature 164, 966 (1949).

8. R. G. Vines, J. Heat Trans. 82, 48 (1960).

9. E. A. Mason and L. Monchick, "Heat Conductivity of Polyatomic and Polar Gases," (to be published).

10. H. F. Calcote, Anal. Chem. 22, 1058 (1950).

III. ROCKET NOZZLE FLUID DYNAMICS

(F. K. Hill, H. J. Unger, S. A. Elder)

Objective

The dynamics of high-speed gas flows in rocket nozzles has become increasingly important to the efficient utilization of high-energy solid propellants. The flow characteristics of the gas mixture are dependent on the thermodynamic properties of the components and certain time-dependent phenomena such as chemical reaction rates, recombination and condensation. Acquisition of the experimental data required for an accurate description of the gas flow from a relatively simple propellant and rocket nozzle combination has been the first objective.

In order to provide realistic and representative testing conditions for the experiment, a double-base solid propellant (ARP)* has been chosen which provides the basic constituents common to most high-impulse propellants. These are hydrogen, nitrogen, carbon monoxide, carbon dioxide and water vapor. Impurities of the order of 2 to 3% are present as is the case in all propellants and it is possible to add in well-controlled amounts and sizes solid particles for future extensions of the experimental studies. To begin with, it is believed advisable to keep the problems as uncomplicated as possible while still retaining the fundamental aspects of the phenomena under investigation. Combustion pressure and temperature of the grain are 1100 psi, nominal, and 2500°K, respectively; end burning is employed for either 10-second or 30-second operation. These conditions are sufficient to introduce measurable

---

* The propellant is manufactured and proof-tested at Allegany Ballistics Laboratory.

measurable effects due to the variable gas properties as the gas expands
through the nozzle, gas non-equilibrium conditions in the expanded flow and
heat transfer and nozzle divergence angle effects. Associated phenomena,
such as erosion and deposition of solid particles, are also present for ob-
servation providing additional data.

It is anticipated that as the work progresses higher specific impulse
propellants will be utilized providing temperature in the $3000°K$ to $4000°K$
range, and that investigations will be undertaken of the effects of metal
additives to the grain and some properties of materials as they are affected
by the rocket gases.

Boundary Layer Measurements

In the previous quarterly report (Ref. 1), boundary layer pressure
profiles were reported for a station in the nozzle where the free stream Mach
number was 4.5. It was indicated that additional measurements of the tempera-
ture profile would be taken in order to provide the data needed from which
velocity profiles could be computed. This was done during the current period
and samples of the temperature and velocity profiles are shown in Figs. III-1
and III-2. The temperature measurements in the stream were made with probes
similar in shape and construction to the pitot probes described in Ref. 1.
Tungsten-iridium thermocouples of 0.005-inch wire were placed inside the en-
trance to the probe and opposite bleed holes to measure the stagnant gas
temperature; the lead wires were insulated by means of alumina ceramic tubing
within the molybdenum probe and shank. The total temperatures measured in
this way are always less than the actual stream value because of radiation
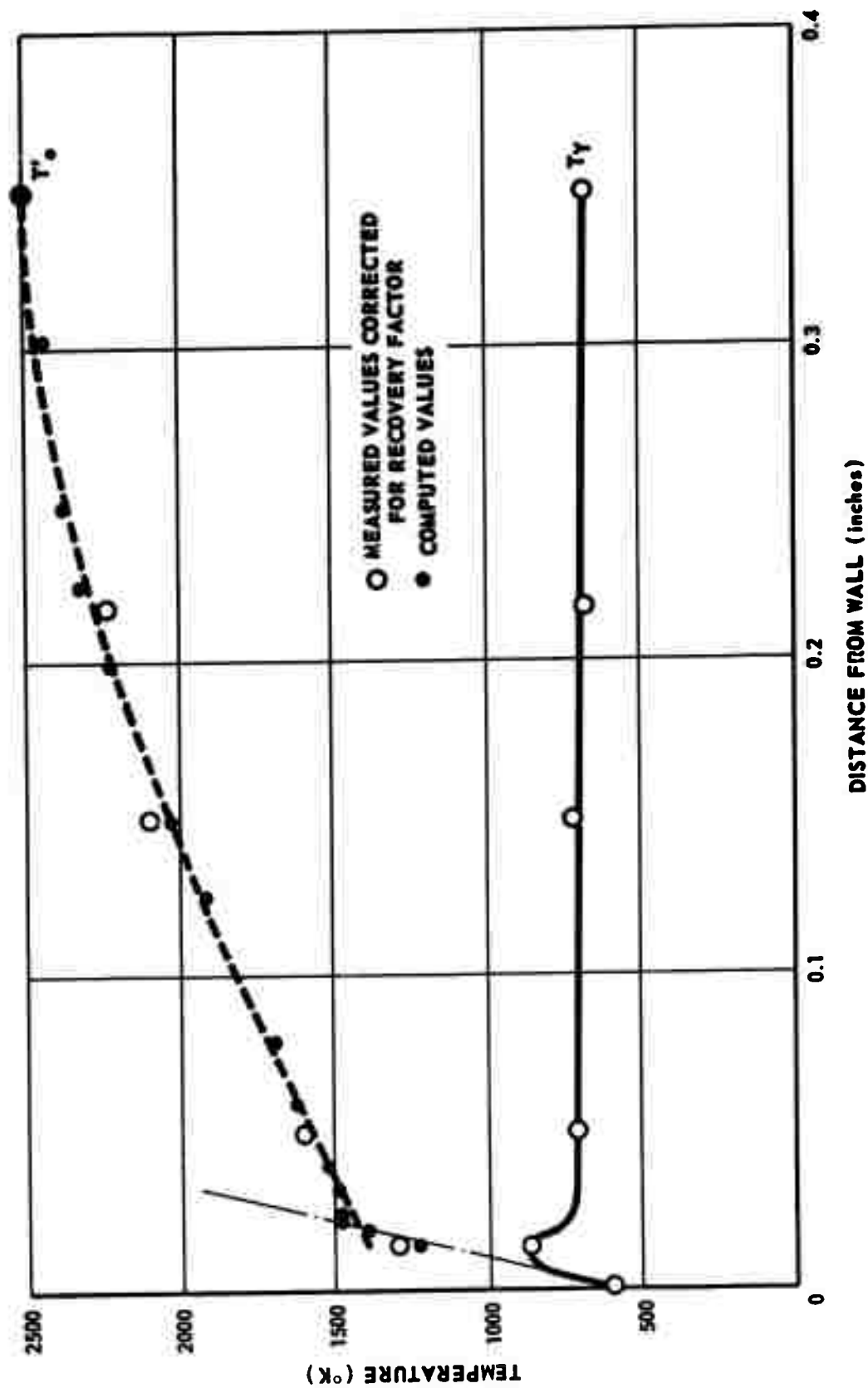losses to the tunnel walls and conductive effects to the supporting structure.

Fig. III-1 TEMPERATURE PROFILE OF BOUNDARY LAYER IN ROCKET NOZZLE
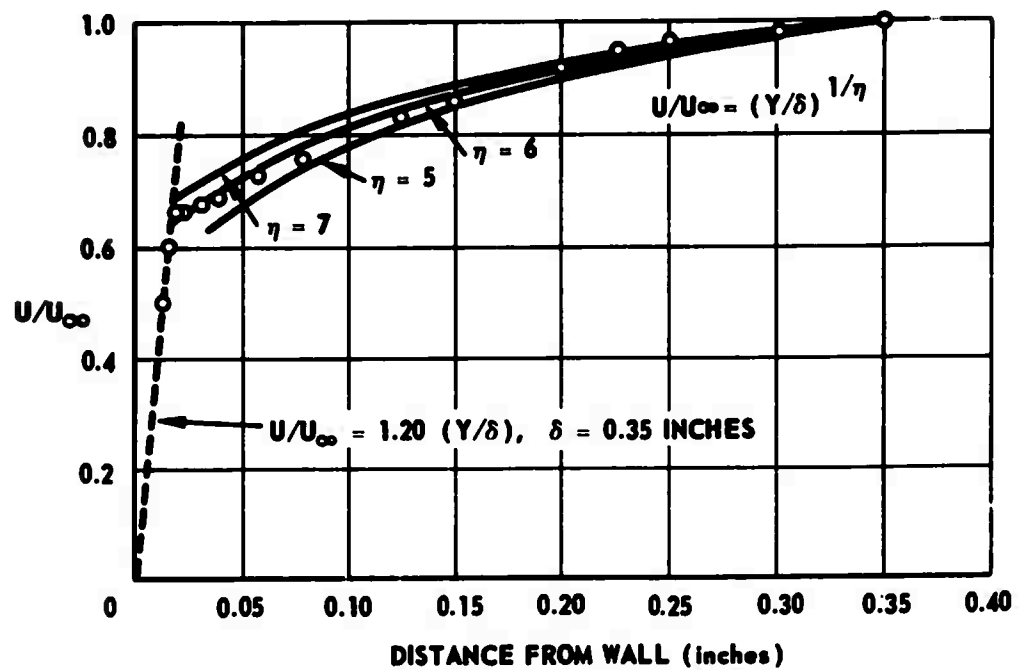MACH NO. = 4.5

Fig. III-2   VELOCITY PROFILE OF BOUNDARY LAYER IN ROCKET NOZZLE
MACH NO. = 4.5

Calibration of the probe recovery factor is accomplished by measuring the total temperature in the free stream and with the known supply temperature computing a recovery factor of the probe. There is some variation of this recovery factor with flow velocity, so that additional measurements are made in a slower speed flow field produced by a choking device in front of one of the probes. This device then produces a calibration on the effective recovery factor for the probe as a function of velocity or Mach number. In our case, the recovery factor varied from 0.834 at M = 4.5 to 0.90 at M = 0.4.

It is noteworthy that the rocket gas mixture exhibits similar characteristics to those of air - the laminar sublayer at the surface, followed by the buffer region, and then the fully developed turbulent section where the velocity index is approximately 5.

Skin friction and heat transfer coefficients are found directly from these data, the latter being of primary interest for heat transfer calculations. The Reynolds analogy between heat transfer and skin friction in the form of the Colburn relation $C_f = 2(St)Pr^{2/3}$ appears to be quite closely approximated by the data. The calculated value of the skin friction, C_f, at this station was 4.33×10^{-4} - the value of the Stanton number 3.09×10^{-4}. The free stream gas mixture properties of viscosity, thermal conductivity and specific heat give a Prandtl number of 0.568. Using these numbers in the Colburn relation yields an agreement of better than 1%.

A survey at a more upstream station has been taken where the free stream Mach number is about 4.3.

Nozzle Development

As mentioned in the introductory statement of objectives, the work is being extended to conditions of higher temperatures. Present combustion temperature of the ARP propellant is 2500°K; a proposed new grain will burn near 3750°K at the same pressure now used (1000 psi). As a result, considerable effort has been devoted to the design of a nozzle suitable for use at this temperature level and of sufficient thermal capacity to permit re-use without suffering deformation or significant throat erosion during 10-second runs. The primary design now ready for fabrication makes use of a relatively thick tungsten insert for the throat region, with carbon downstream for the nozzle surface, plus the backing of various other materials calculated to have suitable mechanical and thermal properties. An alternate approach to that of using highly refractory materials is the use of very highly conductive materials and the provision for efficient convection of heat away from the nozzle surface. This latter approach is being taken by some of the arc jet tunnels where extremely high gas temperatures are involved so that refractory materials are even less desirable because of their relatively low thermal conductivity.

In order to obtain specific data on the heat transfer characteristics of thin-walled highly conductive nozzles compared to the refractory-walled heat-sink types, a test was undertaken in the present rocket tunnel using a copper-lined, water-cooled nozzle. The heat transfer results thus obtained were directly comparable to the heat-sink type of nozzle made of highly refractory material which have been in use for some time and on which a fairly complete inventory of heat transfer properties has been accumulated. Fig. III-3 shows schematically the geometry of the two types of nozzles.

COOLING WATER
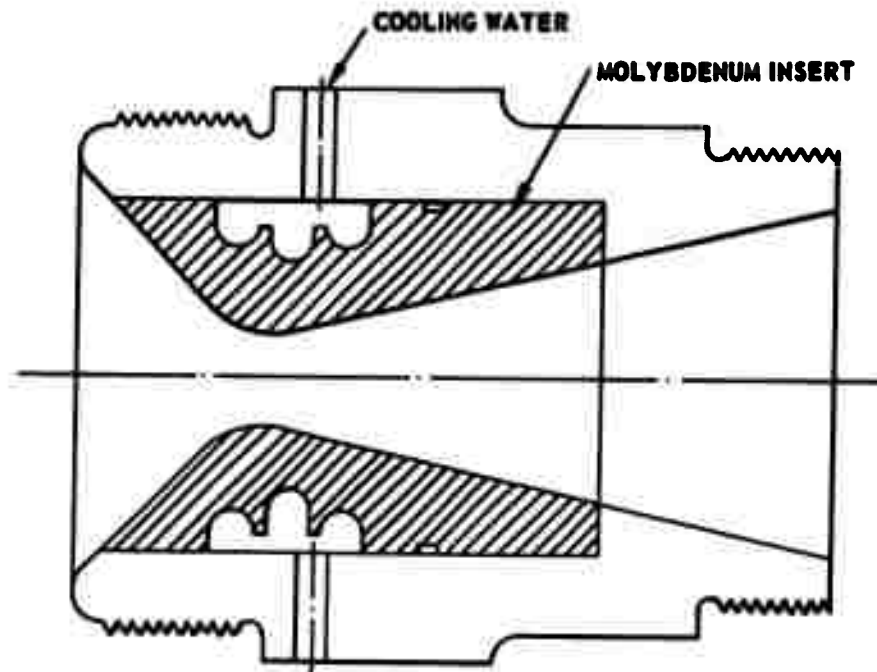
MOLYBDENUM INSERT

CONVENTIONAL MOLYBDENUM INSERT NOZZLE

COOLING WATER:

OUTLET   INLET   OUTLET
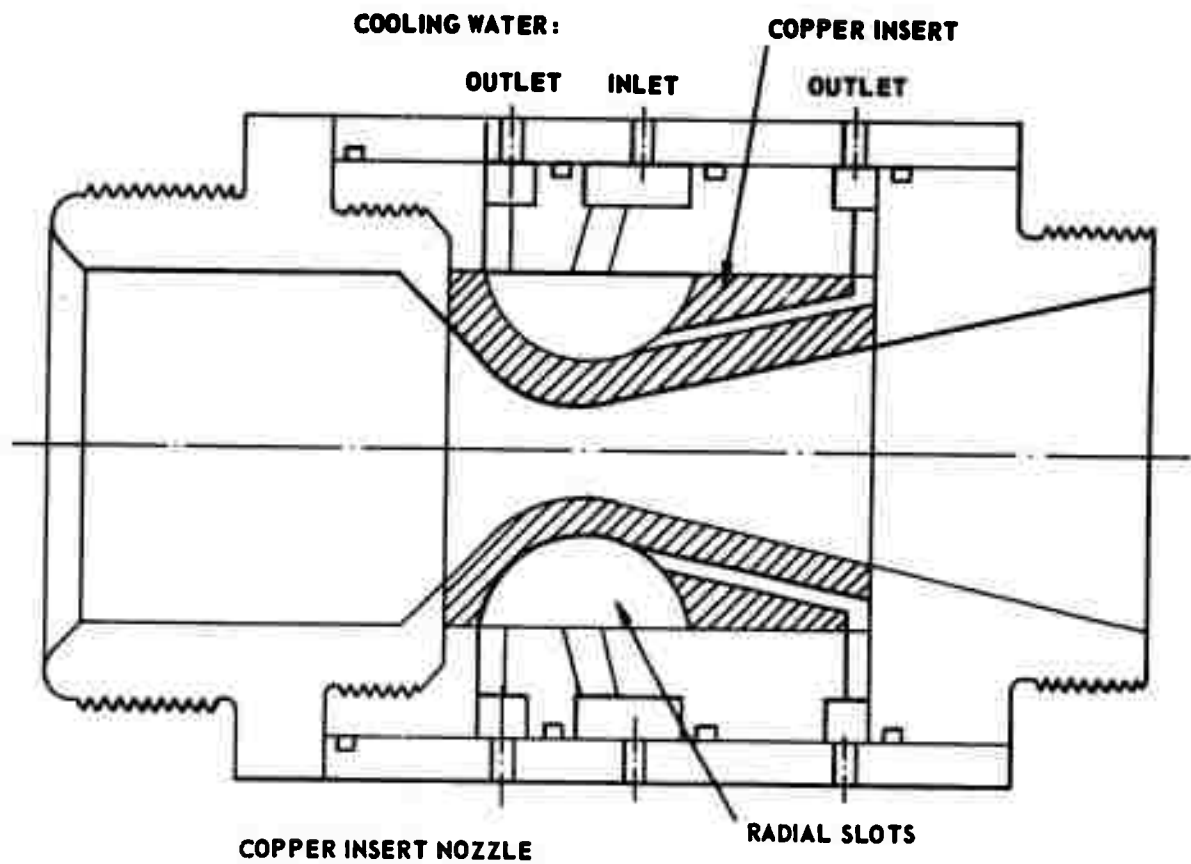
COPPER INSERT

COPPER INSERT NOZZLE   RADIAL SLOTS

Fig. III-3   SCHEMATIC OUTLINES OF NOZZLES USED FOR HEAT TRANSFER
MEASUREMENTS

A test run with the copper-lined nozzle indicated that, in the area defined by the copper section, more than two times the heat was transferred as compared with the refractory nozzles. Peak heat transfer rates at the throat with a molybdenum insert were from 2 to 3 BTU/in^{2}sec; with the copper liner, the average over the entire area of copper was above 5 BTU/in^{2}sec. This result illustrates the increase in heat transferred to the nozzles when the surface temperature is maintained at a low level (throat temperature for the Cu $\sim$ 500°, for Mo $\sim$ 1600°K) so that the value of the gas temperature gradient at the surface is large. The heat transferred at any point is $k \frac{dT}{dy}$ where k is the gas thermal conductivity and dT/dy the temperature gradient at the wall. Thus for a given free stream temperature, dT/dy will increase as the wall temperature decreases, the value of k remaining relatively constant.

Spectroscopic Developments

In last period's report the "noise" problem was discussed and several modifications to the infrared scanning spectrometer described. These changes were all found to be necessary to reduce mechanical vibrations induced by the high airborne sound level during rocket operation. The "noise" signals, however, were still not eliminated and so during this period primary emphasis was placed on this problem.

Five rocket tests were used as sound sources for observing changes in the signal to noise ratio produced by electrical and mechanical changes in the spectrometer. A sixth test used the tunnel nozzle as the absorption cell to see if the changes actually improved over-all operation.

To begin with, the spectrometer was reassessed for the purpose of eliminating as many sources of vibration as reasonably possible. During this

process the optics were realigned and the resolution greatly improved. The
slits were set at approximately 100μ and a PbSe detector used, giving a
signal to noise ratio at 4μ of at least 100. Test No. 128 showed no apparent
improvement during operation of the rocket motor (see Fig. III-4). It ap-
peared that the noise amplitude during operation was independent of the signal
amplitude, which suggested that the noise was generated in the detector and its
associated amplifier. Setting the detector on one inch of felt made no im-
provement, indicating that most of the vibration was caused by airborne noise.
Fig. III-5 shows the output of the detector and preamplifier only during a run,
Test No. 129. The usual illuminating source was turned off to eliminate it and
the monochromator as noise sources. The resulting trace, although small in
amplitude, clearly shows the spurious noise signals. Fig. III-6 was made during
Test No. 130, with a felt pad under the detector mount. With this in mind, an
attack was made on the entire detector system.

The rubberband shock mount of the detector Dewar flask was replaced by
a tightly fitting Selastic cylinder and the emitter follower was potted in a
block of aluminum. All switches and mechanical connections were replaced by
soldered joints. Test No. 131 was made with the spectrometer in operation with-
out a light source and, as Fig. III-7 shows, there was still electro-mechanical
noise present.

Fig. III-8 shows a spectrogram taken through the tunnel absorption
cell during Run No. 132. The noise signal still seems to be independent of
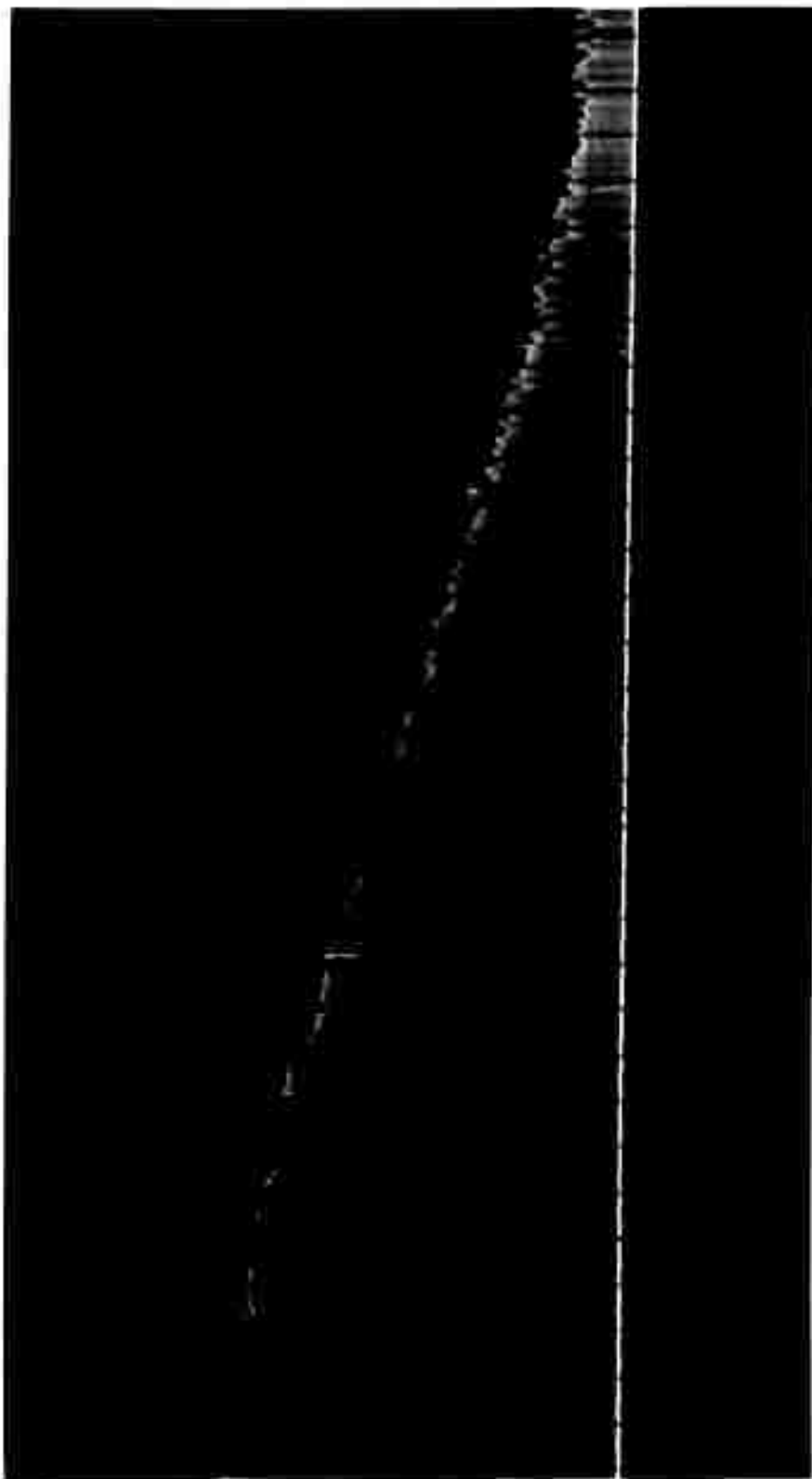signal amplitude, indicating that the origin is in the detector system.

Fig. III-4 SCANNING SPECTROMETER RESPONSE DURING RUN NO. 128

A one-inch thick felt pad was placed under the
spectrometer to damp vibrations transmitted over
the optical bench to the monochromator and
detector.

Fig. III-5 OUTPUT OF DETECTOR AND PREAMPLIFIER ONLY DURING TEST NO. 129
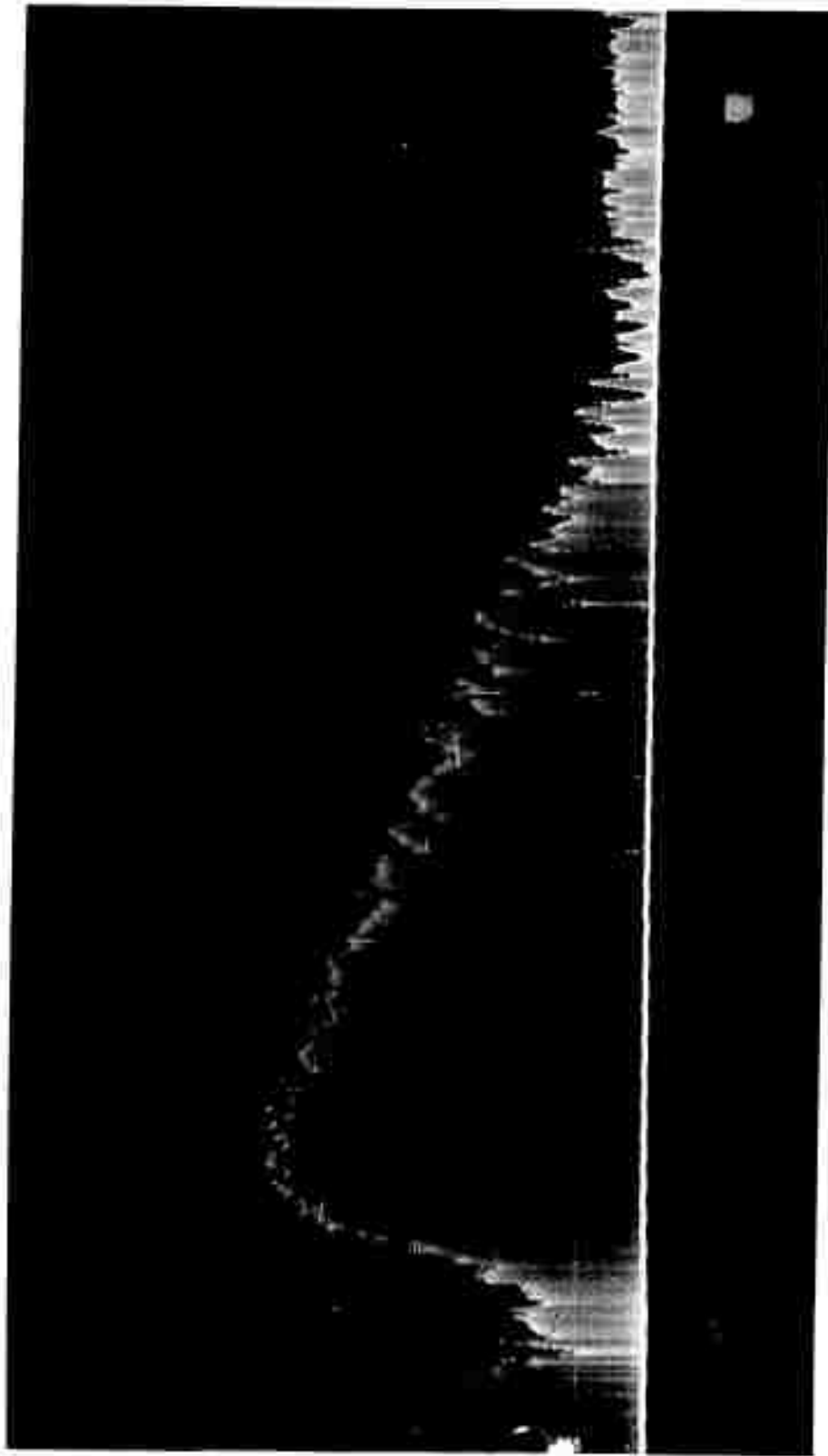
Source and monochromator section eliminated.

Fig. III-6 SPECTRAL RESPONSE DURING TEST NO. 130

A felt pad was placed under the detector mount
and the switch in the preamplifier (supplying
power to the transistors) was bridged by
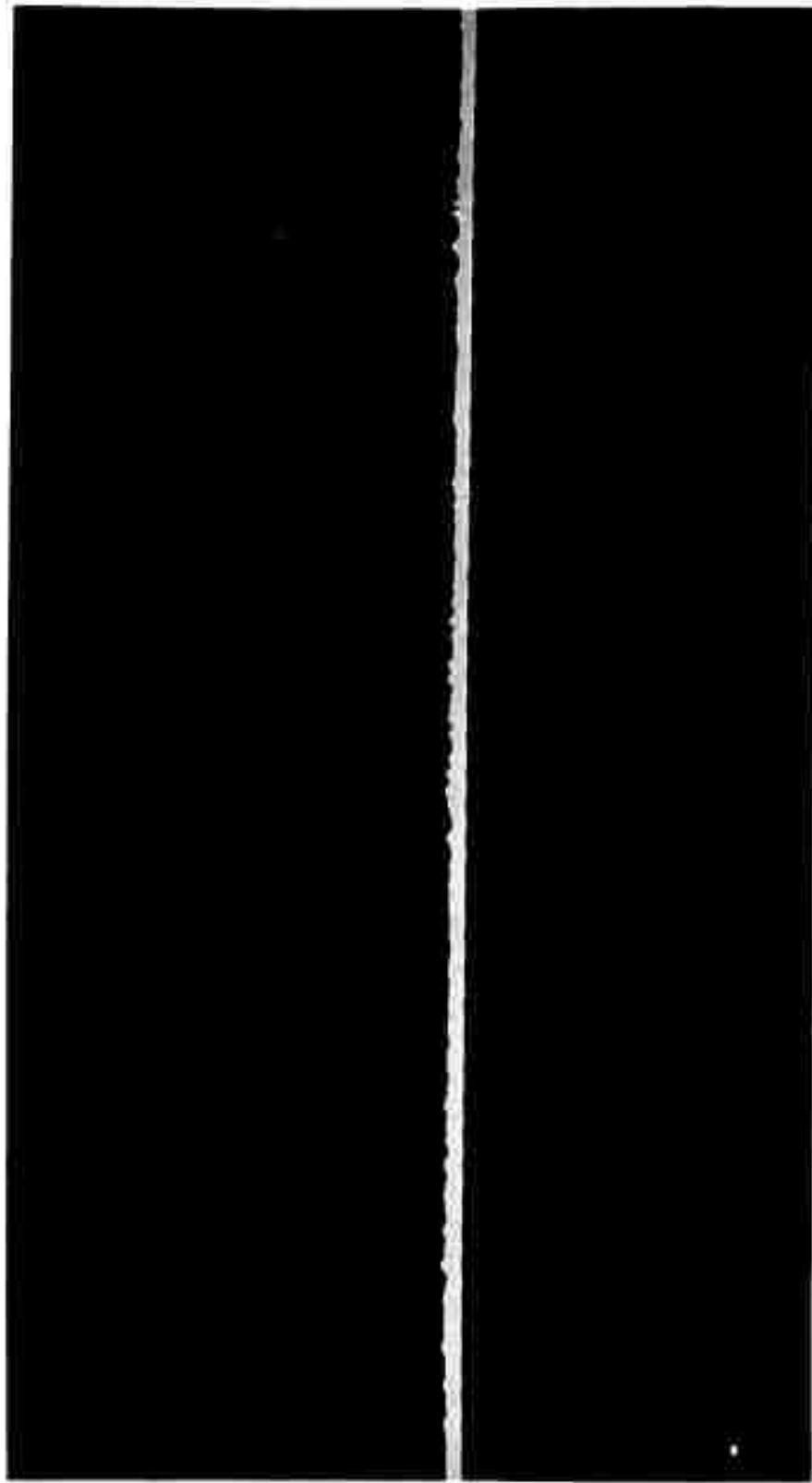soldered connections.

Fig. III-7 SIMILAR TO FIG. 5, BUT WITH A PREAMPLIFIER POTTED IN A
MECHANICAL ALUMINUM CASE ELIMINATING ALL CONNECTORS AND
IMBEDDING THE DETECTOR IN A SELASTIC CYLINDER TO
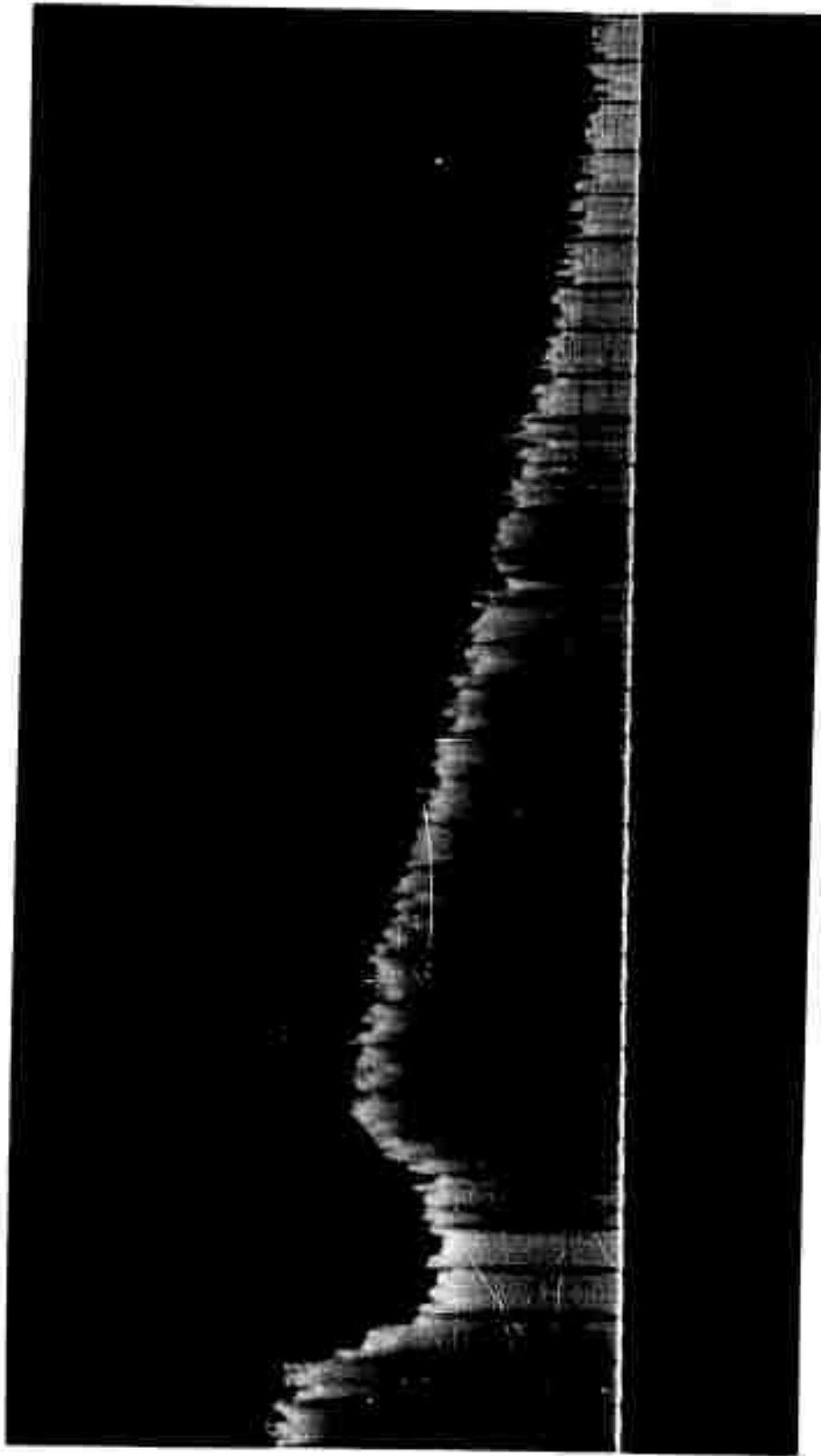REDUCE MICROPHONIC NOISE

Test No. 131.

Fig. III-8 SPECTRUM OF TUNNEL CELL DURING TEST NO. 132

Previous modifications included and a bakelite flange
placed under the detector to electrically isolate it.
Numerous lead weights placed on the housing of the
spectrometer to reduce possible movement.

Since the resolution of the spectrometer is better than needed for practical absorption measurements, the signal to noise ratio can be increased by opening the spectrometer slits and reducing the amplifier gain. Fig. III-9 shows a spectrogram taken in Test No. 133 without flushing the spectrometer with dry air to remove the atmospheric absorption. The slits have been opened from 100μ to 170μ in this test and the signal increased five times. It appears that with slit widths of the order of 200μ the signal to noise ratio will be adequate for quantitative measurements to be made under the test environment.

Temperature Measurement

In a previous ARPA report (Ref. 2), progress was described in the development of a transistorized brightness pyrometer. This device was developed to supplement the two-color pyrometers in the lower temperature range (below 1400°K). For the first version of the pyrometer, shown in Fig. III-10, the design emphasis was on simplicity, since it was felt that the reliability of the instrument would be enhanced by having as few parts as possible. The control box was designed to be hand-held and is ordinarily separated from the test area by a 50-foot cable. The output of the control box may be fed directly to a dc oscillograph. Figure III-11 shows a schematic of the optical system.

The electronic circuits are shown in Fig. III-12. The optical box circuit contains only seven components, including the phototransistor and battery. The phototransistor, connected in common emitter mode, requires no preamplifier.

The control box circuit comprises a decade amplifier and demodulator as shown in Fig. III-12. Gain stability is assured by the application of 34 db of feedback via the 18Ω series feedback resistor. A diode demodulator is
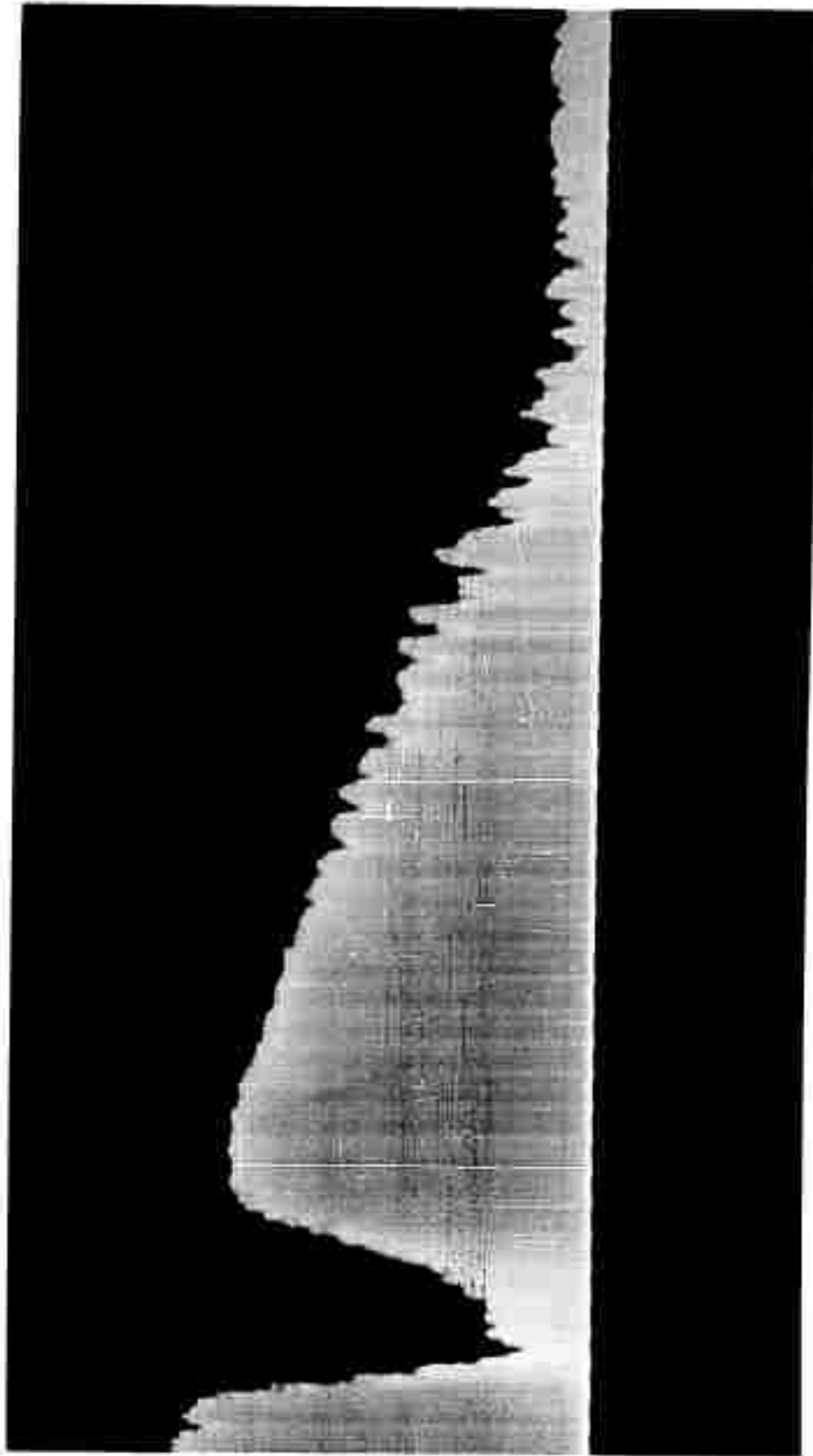
Fig. III-9 SPECTRUM OF ATMOSPHERIC ABSORPTION DURING TEST NO. 133

The slit width was increased from 100 μ to 170 μ reducing the
resolution but increasing the signal to noise ratio. (The
signal was increased five-fold).
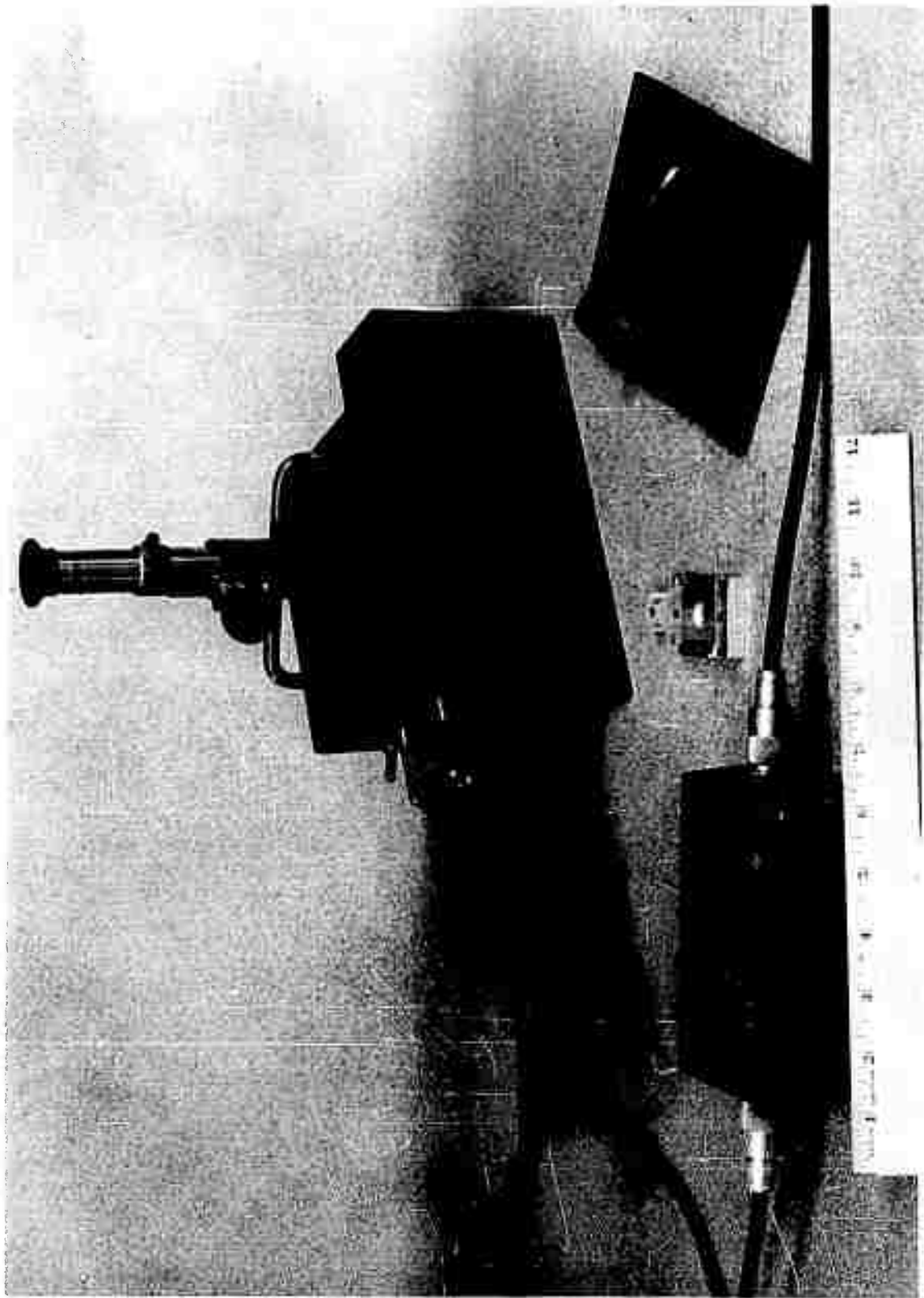
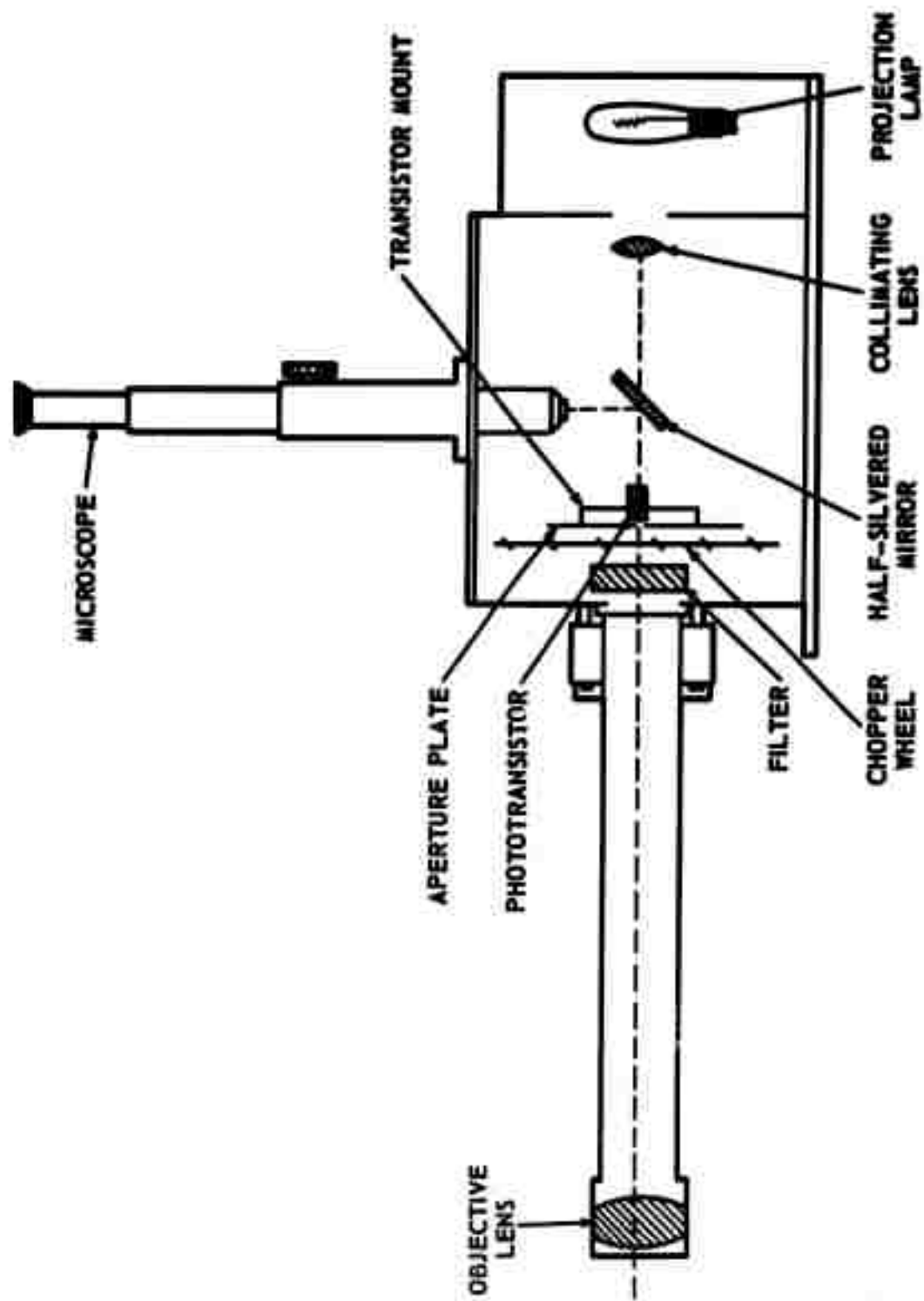Fig. III-10 FIRST VERSION OF PHOTOTRANSISTOR PYROMETER

Fig. III-11 SCHEMATIC OF OPTICAL SYSTEM OF PHOTOTRANSISTOR
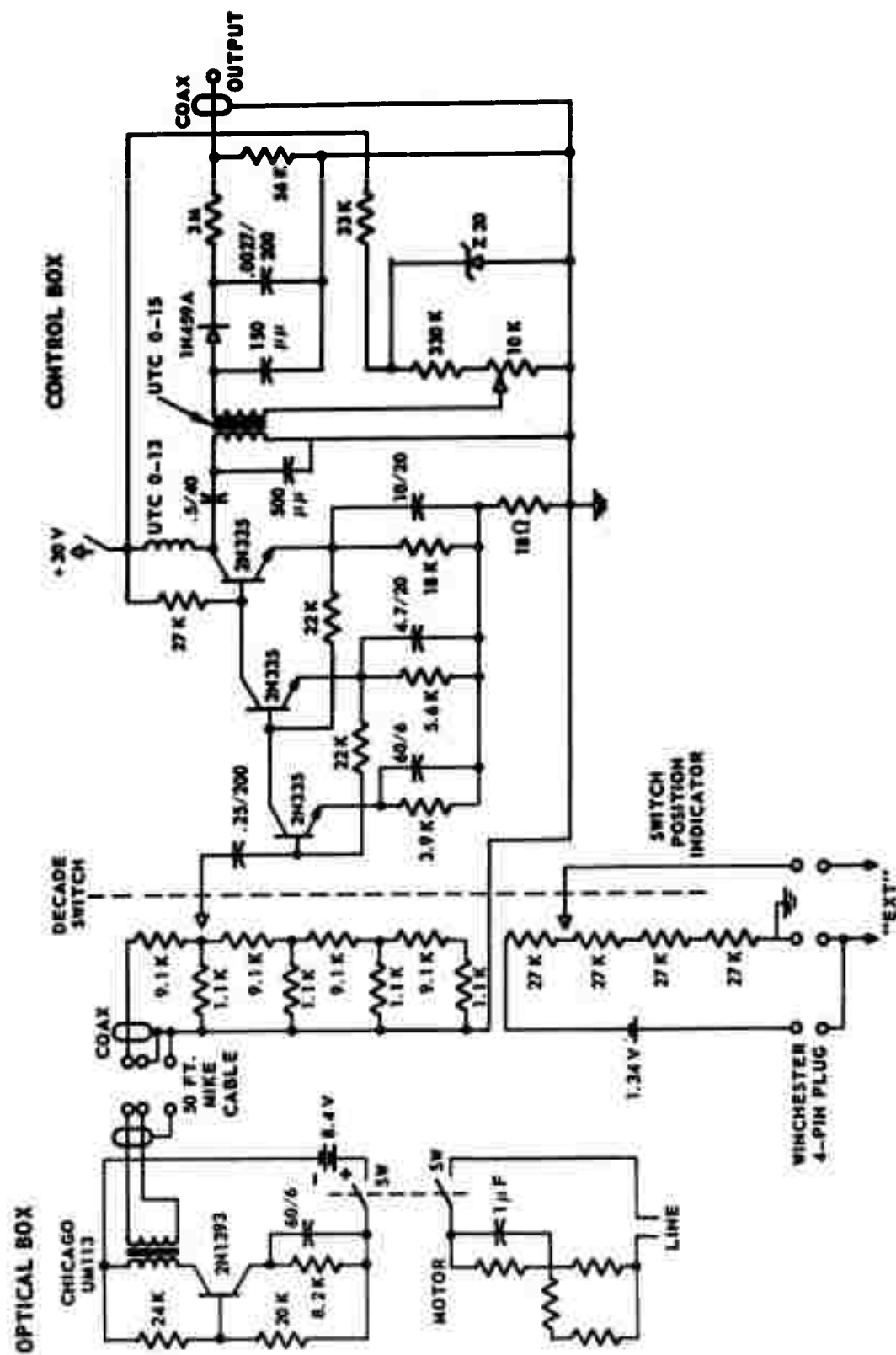PYROMETER NO. 1

Fig. III-12 CIRCUIT DIAGRAM FOR PHOTOTRANSISTOR PYROMETER NO. 1

transformer-coupled to the last transistor stage to give dc output for recording on an oscillograph. Output signal level for full-scale deflection of the oscillograph pen is 250 mv dc, corresponding to a line input of 2.5 mv rms. Noise level referred to the input of the decade amplifier is about 50μv rms at maximum gain.

By means of the decade attenuator, a large linear dynamic range (about 4000 x referred to noise level) can be attained, the upper limit being imposed by clipping in the phototransistor. The dynamic temperature range of the pyrometer as a whole is affected partly by the dynamic voltage range of the electronic system and partly by the efficiency of the optical system. This is shown in Fig. III-13 where typical calibration curves are plotted on log-reciprocal axes. The temperatures given are "black body" temperatures (i.e., corrected for the emissivity of the tungsten calibration lamp).

With wide open telescope objective (Curve C), the "linear" range extends from about 725°K to about 1400°K. By stopping down the telescope opening, the temperature range may be shifted upwards as shown in Curve B, where it extends from 950°K to 3000°K. The straight line portion of the curve corresponds to the linear portion of the electronic dynamic range. Over this region the output signal is very nearly proportional to the light intensity, which, in accordance with Wien's Law, varies exponentially with reciprocal of the absolute temperature. The slope of the straight line portion depends on the center wave length of the bandpass of light being received, as may be seen in Curve A. Here, a light filter with center wave length in the visible spectrum was used in place of the infrared filter.
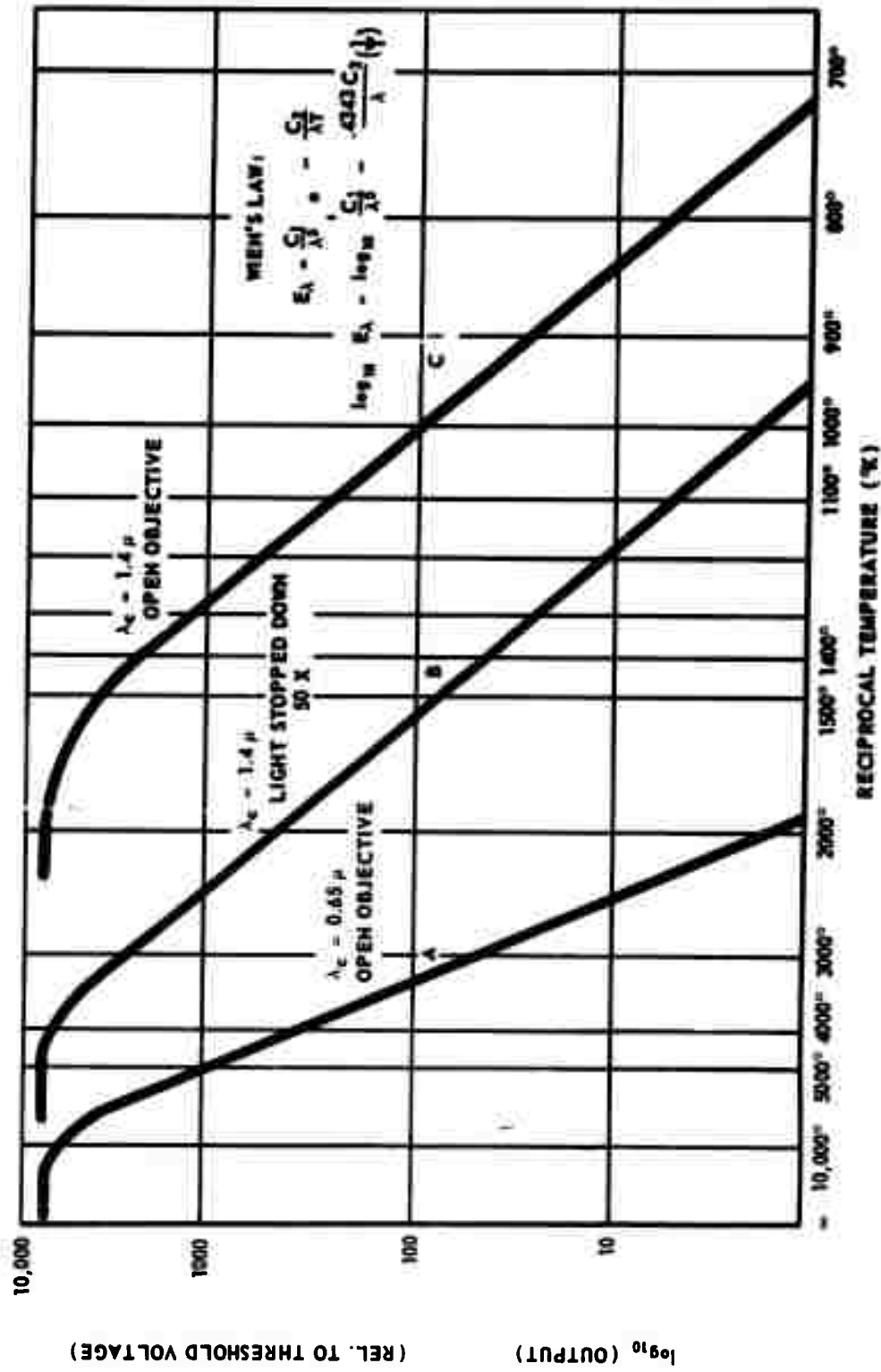
Fig. III-13 TYPICAL CALIBRATION CURVES FOR PHOTOTRANSISTOR PYROMETERS

Actually, the phototransistor current is not quite proportional to input light intensity so that the slope of the calibration curve is off by a few per cent from that which would be expected from Wien's Law. For the particular phototransistor used, at ambient temperature of about 70°F, the output current varies as the 1.1 power of the input light intensity.

The chief advantages of the pyrometer system described above are its nearly complete freedom from sensitivity to shock and vibration, and its compactness. It is also relatively inexpensive to build, the total cost of parts being under $100.00. Its precision is fair, having a calibration reproducibility of about ±10°C under ordinary laboratory conditions.

The chief disadvantage is that the response of the phototransistor varies somewhat with ambient temperature. Since both the slope and theshold abscissa of the calibration curve are affected by changes in ambient temperature, the pyrometer needs to be calibrated under conditions identical to that in which it is to be used for best accuracy. This is not always a convenient procedure for field use.

To get around this problem, a second version of the pyrometer has been developed in which the electro-optical response of the phototransistor has been stabilized by means of "photofeedback". The photofeedback is accomplished by means of a subminiature tungsten-filament light bulb* flush-mounted on the window of the phototransistor as shown in Fig. III-14. The complete circuit is given in Fig. III-15. Here, the phototransistor becomes part of a direct coupled common emitter cascade. Base bias for the phototransistor is supplied

---

* Kay Electric Company Type 15-15 "Pinlite".

Fig. III-14 CLOSE-UP OF TRANSISTOR MOUNT FOR PHOTOTRANSISTOR PYROMETER
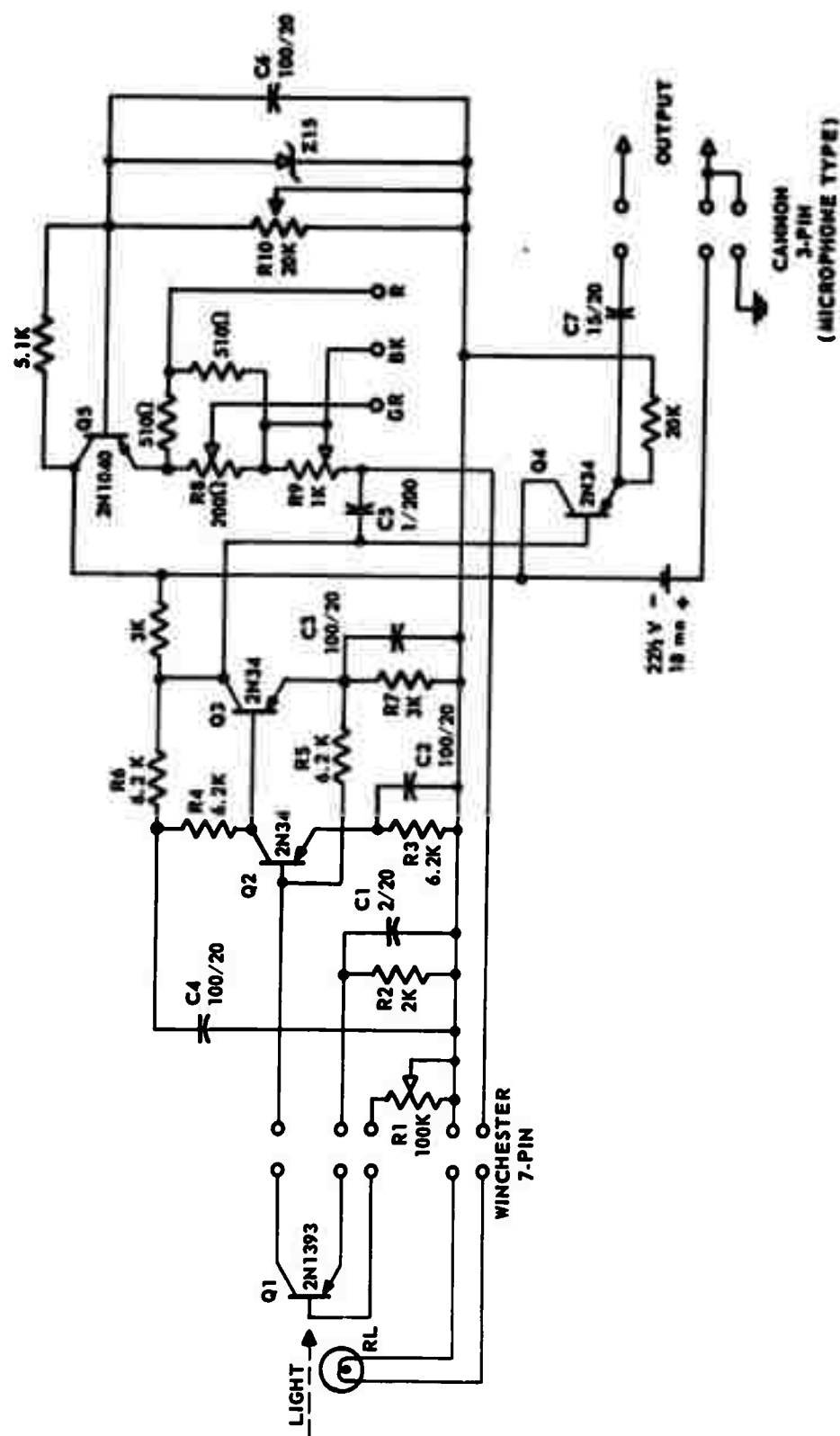NO. 2 SHOWING FLUSH-MOUNTED SUBMINIATURE FEEDBACK LAMP

Fig. III-15 PHOTOFEEDBACK AMPLIFIER CIRCUIT - PYROMETER NO. 2

by the dc component of the light from the feedback lamp, which is itself biased at a steady 12 ma current so as to have linear transducer response. The need for wide band amplifier response was eliminated by mechanically chopping the light beam into a sine wave rather than the usual square wave. This was accomplished by placing the chopper blades close to the plane of the objective lens and making the lens aperture equal to blade width. The optical system is shown schematically in Fig. III-16. The phototransistor was mounted at the rear of the box. A 180 cps chopping frequency was chosen to place the signal in the pass band of the amplifier.

The decade amplifier employed with the original pyrometer was found to be unsuitable for the photofeedback version, since it did not have enough feedback at low frequencies. The circuit was modified by removing the output transformer and load inductor as shown in Fig. III-17. In order to obtain linear operation of the detector without a step-up transformer, it was necessary to operate at higher supply voltage. A "boot strap" emitter follower stage was added as an output buffer to improve the circuit stability.

The use of photofeedback in the second version of the pyrometer has resulted in greater precision as well as greater calibration stability. The voltage calibration of the feedback version is reproducible to better than 1%, resulting in a temperature reproducibility of better than $\pm 1°C$ at 1000°K and $\pm 4°C$ at 2000°K. In principle, the precision could be improved even further by redesigning for a greater amount of feedback, although the stability of the feedback lamp characteristics may impose a practical limit. The threshold temperature is about 840°K (as compared with 725°K for the non-feedback version). The big advantage of the feedback pyrometer is that after an initial "absolute" calibration using a standard black body, it does not need to be optically calibrated again. This makes it ideal as a field instrument. Another advantage is
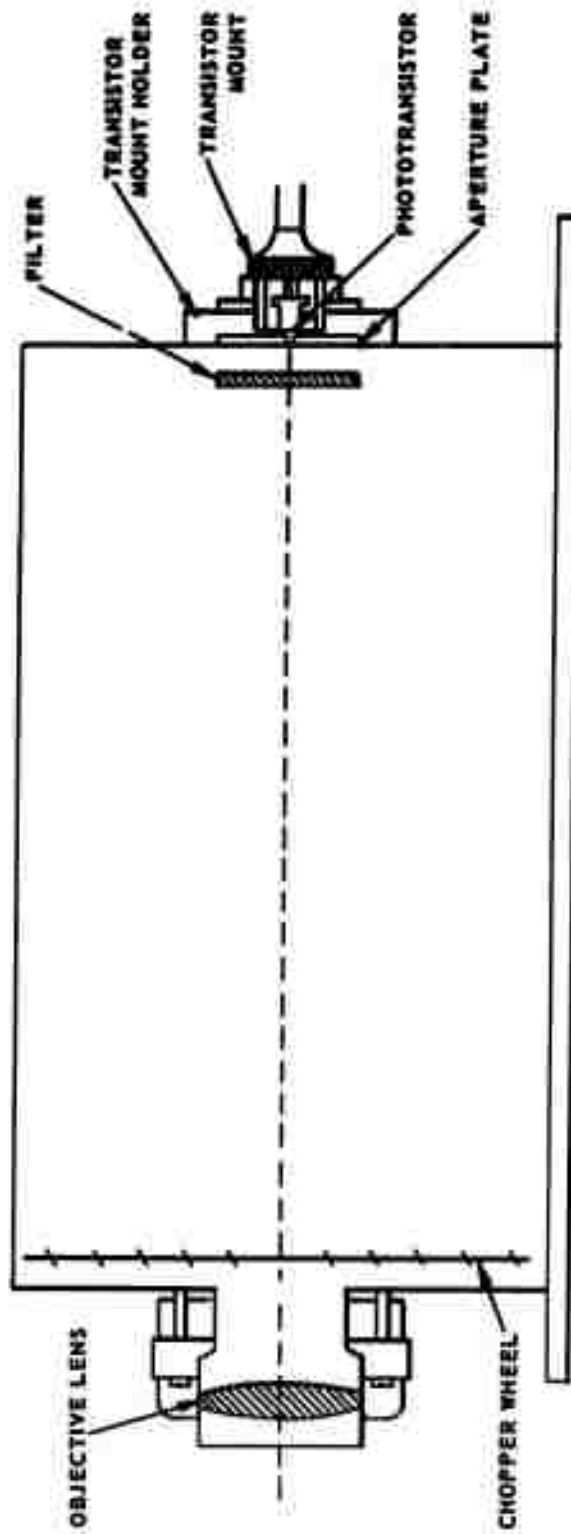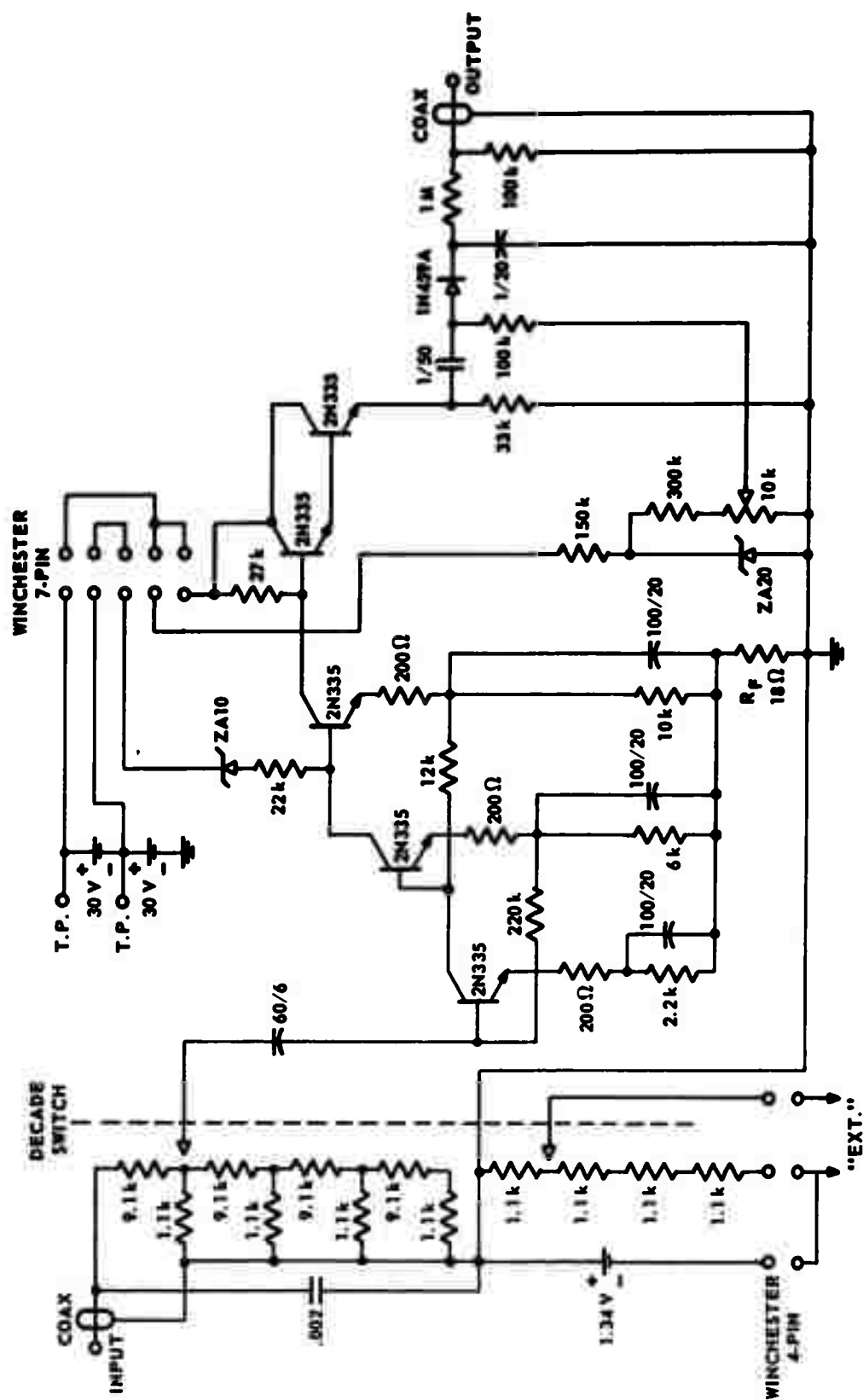
Fig. III-16   SCHEMATIC OF OPTICAL SYSTEM OF PHOTOTRANSISTOR
PYROMETER NO. 2

Fig. III-17 CONTROL BOX CIRCUIT FOR PHOTOFEEDBACK PYROMETER

that the feedback improves the linearity of the phototransistor response. The photofeedback principle ought to be useful for photometric devices in general.

At the present stage of development, the non-feedback pyrometer has some advantages of its own: It works at higher chopping frequency, has somewhat better threshold sensitivity and dynamic range, and is less affected by microphonic pickup in severe vibration environments. Refinements in the photofeedback circuitry, however, may neutralize these differences. Both instruments are currently being used in rocket tunnel experiments.

Recently, several attempts have been made to measure the throat surface temperature through a 0.060-inch hole in the wall of the nozzle. In each case there seems to have been some attenuation of the light from the throat during the course of the run. To find out whether this might be due to thermal expansion of the nozzle (causing optical misalignment), the following experiment was done: A subminiature lamp, similar to that used in the photofeedback pyrometer, was taped on the side of the nozzle flange. One of the pyrometers was then mounted on the optical bench as usual and aligned to focus on the lamp. Any change in alignment was then immediately detectable as a change in signal level of the pyrometer. By this means, it was possible to measure the motion of the flange to a precision of better than 0.001 inches. The position trace obtained in this way (for Test No. 134) is shown in Fig. III-18. The observed amount of motion is indeed enough to account for the discrepancies of earlier experiments. That the motion was due entirely to thermal expansion is indicated by the fact that the flange was found to return to its original position again after the apparatus had had time to cool.
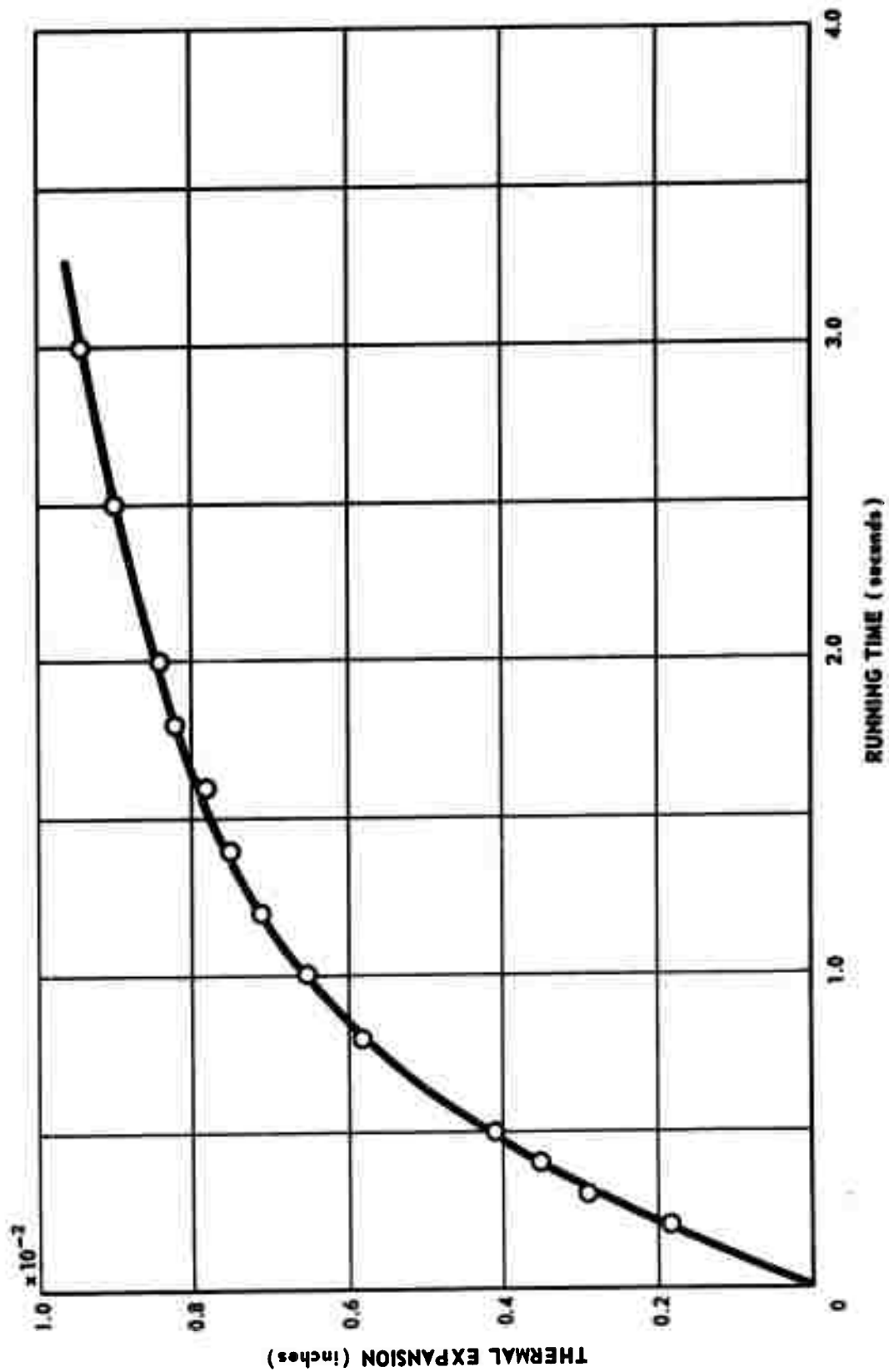
Fig. III-18   MOTION OF NOZZLE FLANGE CAUSED BY THERMAL EXPANSION
DURING TEST NO. 134

Some thought is being given to the possibility of maintaining pyrometer alignment in future tests by means of a servomechanism.

References

1. Task R Quarterly Progress Report No. 9, APL/JHU TG 331-9.

2. Task R Quarterly Progress Report No. 7, APL/JHU TG 331-7.

IV. ROCKET NOZZLE CHEMICAL KINETICS

(A. A. Westenberg and S. Favin)

Objective

Aerodynamics and chemical kinetics are strongly coupled in the
flow of most propellant gases through an exhaust nozzle. Understanding
of this interaction and the ability to predict its effects must be
founded solidly on the fundamental chemical processes involved. In all
cases of practical importance, these basic processes are exceedingly
complex. As a result, all of the theoretical work which has been done
in this field has been confined to more-or-less idealized, simplified
chemical systems - generally of the diatomic molecule dissociation-
recombination variety. Even in these cases the analytical and compu-
tational problems are formidable, and various approximations have been
proposed for dealing with the situation. The utility of these approxi-
mations in the more complex flows typical of real propellants remains
to be established. The aim of this work is to apply the results of
other phases of the Task R program, as well as work done elsewhere,
and examine the complex chemical kinetics occurring in the flow of real
propellant gases through nozzles with a view to determining if and when
various simplifying procedures are valid.

Results of Numerical Calculations

The previous quarterly report (Ref. 1) contained a discussion of
the appropriate equations for numerical solution of the flow in a nozzle
with several chemical reactions occurring. The inlet conditions chosen

for the particular case being studied were outlined. It was pointed out that difficulties in starting the numerical solution from an equilibrium condition at the inlet had so far prevented the full problem from being solved.

Since no such trouble was encountered in a partial solution in which it was assumed that the H and OH radicals were equilibrated everywhere, this approximation was treated first. Iteration was performed for the correct mass flow variable A_t/m, and the solution passed smoothly through the throat with a convenient value of the precision index. This solution is designated "3-body equilibrium" in the accompanying figures. Both 12.5° and 25° nozzles were calculated.

The 3-body equilibrium solution at a point slightly downstream of the throat ($z = 2.70246$ cm) was then used as a starting point for an integration of the complete problem. Since this was a non-equilibrium starting point, the integration was apparently initiated with no trouble. It is of interest to note that the whole distance in the nozzle out to $z \cong 20$ was accomplished in a time of only 5 minutes on the IBM 7090. This is in marked contrast to problems encountered in other work of this type (Ref. 2) where the main obstacle to carrying out solutions with several reactions was the exorbitantly long machine time required even on comparable machines. It is not clear whether most of the difference lies in the form of the equations used, or simply in the integration precision required.

In addition to the foregoing two solutions, both frozen and equilibrium flows were calculated. These are included in the accompanying figures.

Discussion

In comparing results of calculations like this where different assumptions about the chemistry are involved, it should be borne in mind that it is not possible to have the different cases all start from the same inlet conditions (static temperature and pressure and gas composition) and also have the same mass flow parameter A_t/m. The latter is unique in each case, so that small variations in this quantity alone lead to slightly different flow profiles. For this reason it would be preferable to perform such comparisons starting from the same initial conditions in the supersonic expansion part of the nozzle only. In this way the mass flow could be kept the same and small differences of interest would not be obscured by this side effect. Future calculations will be done in this way. This also avoids the need for tedious iteration for the mass flow parameter.

The second point to note in these specific examples is that the full problem was solved only from the throat and beyond using the 3-body equilibrium solution to start. If the full problem could have been carried out from the chamber the result would have been somewhat different in detail but not in the over-all conclusions.

Figs. IV-1 to IV-4 summarize the results of calculations on the 25° total angle nozzle. The static temperature profiles with distance down the nozzle are shown in Fig. IV-1 for the four cases treated, i.e., frozen composition, equilibrium, the 3-body equilibrium approximation, and the exact chemical kinetic solution. It is immediately obvious that the exact solution is far from the equilibrium flow limit and, so far as
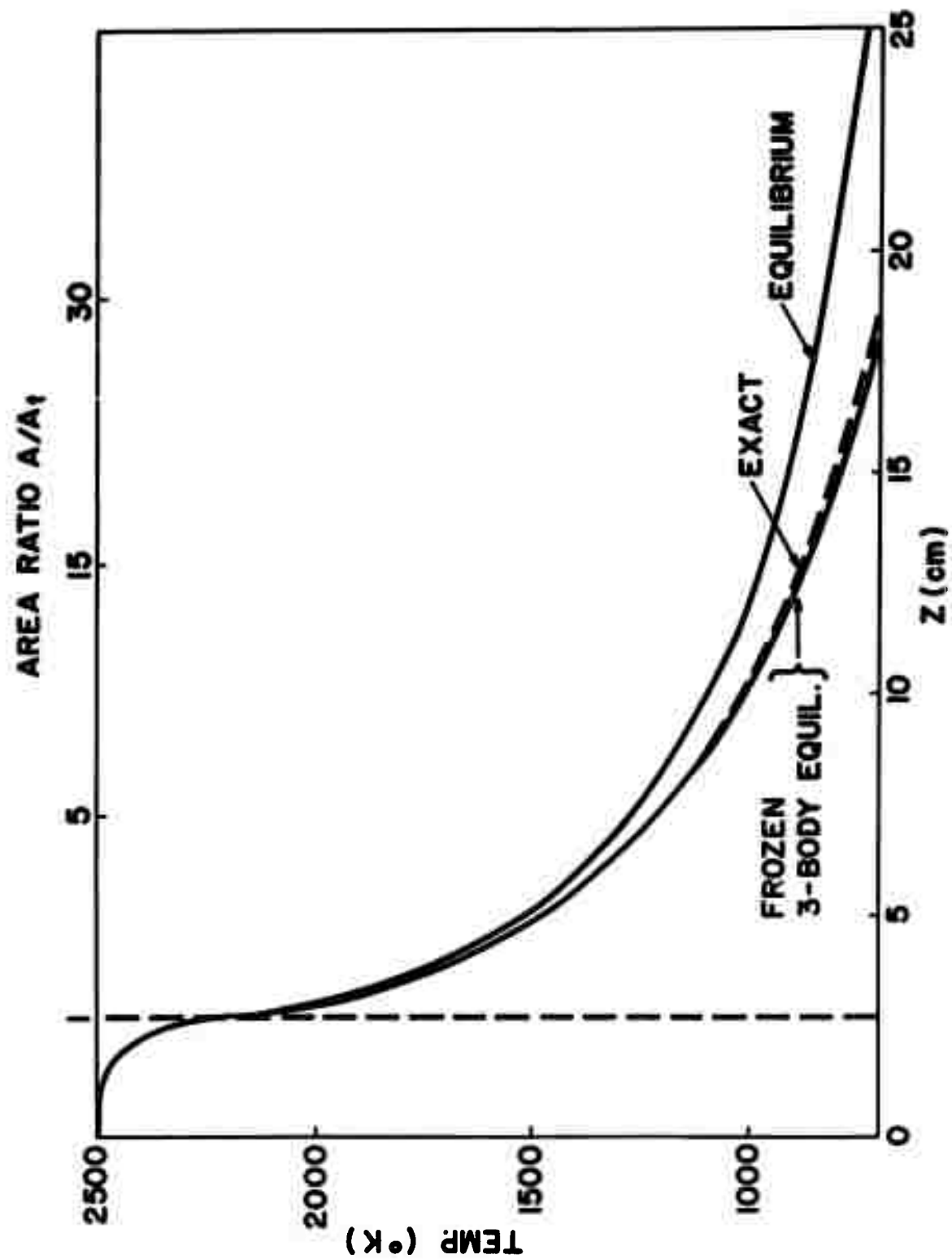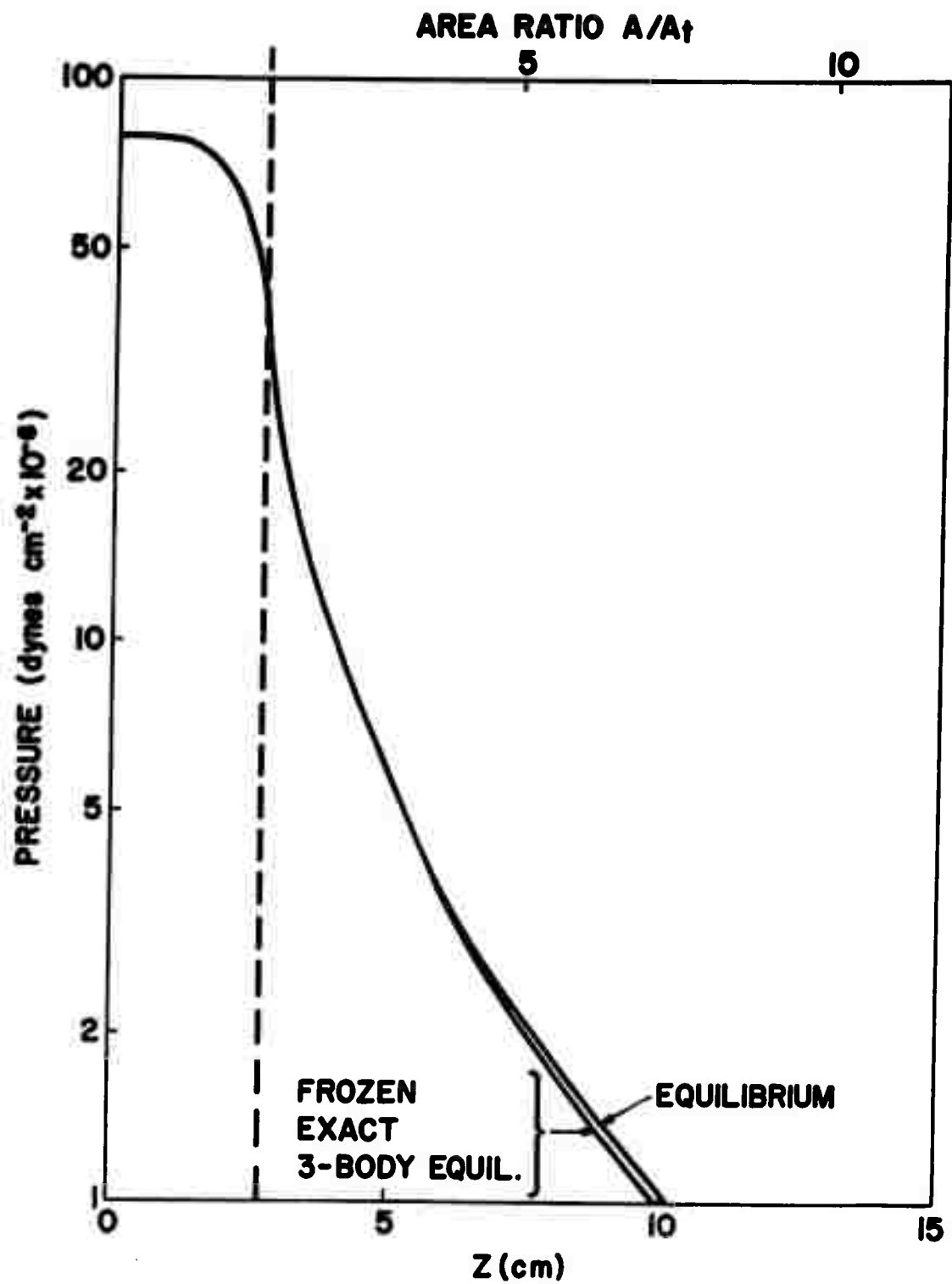
Fig. IV-1 CALCULATED STATIC TEMPERATURE VERSUS DISTANCE IN A 25° TOTAL ANGLE NOZZLE

Fig. IV-2   CALCULATED STATIC PRESSURE VERSUS DISTANCE
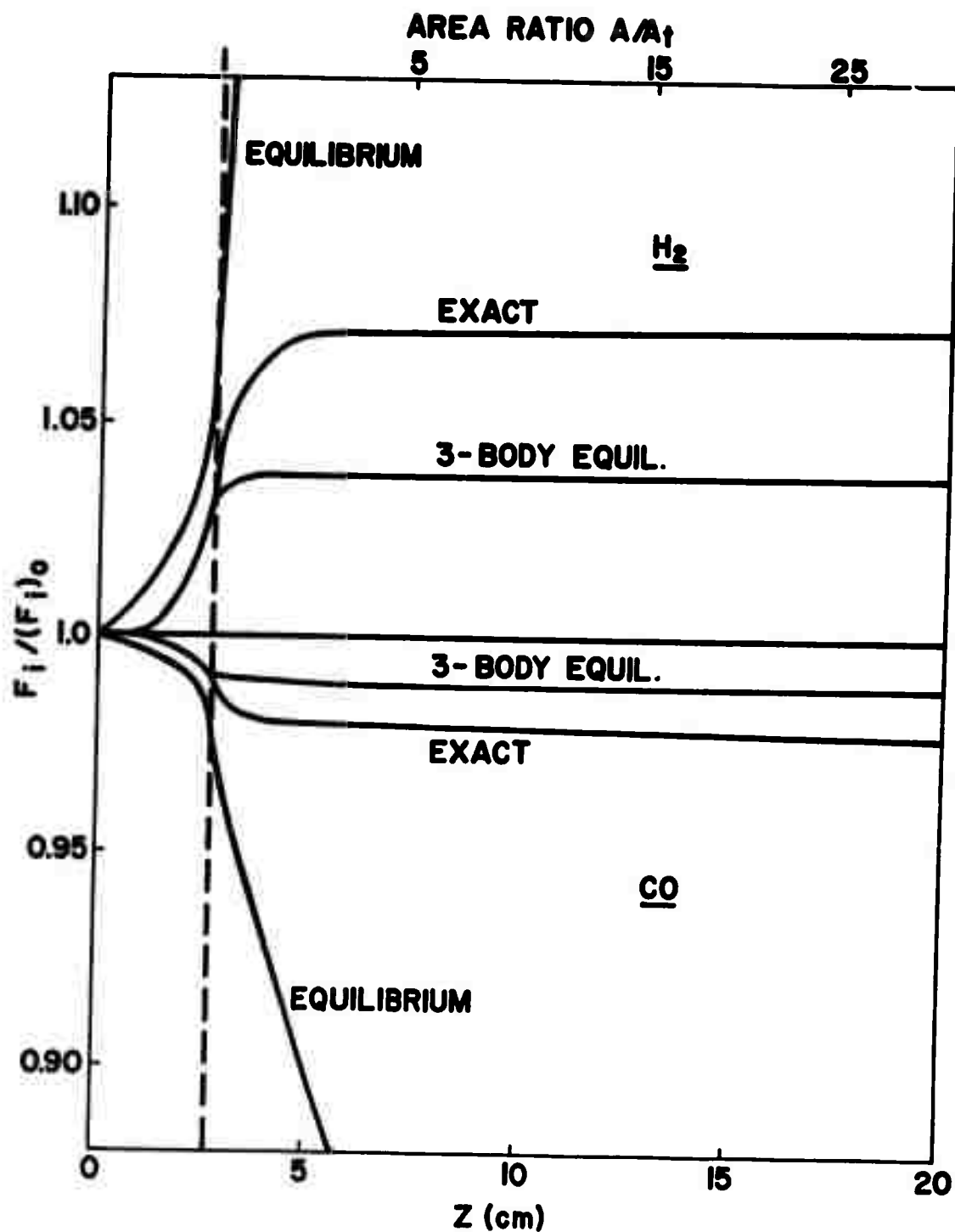IN A 25° TOTAL ANGLE NOZZLE

Fig. IV-3 CALCULATED SPECIES CONCENTRATIONS VERSUS DISTANCE
IN A 25° TOTAL ANGLE NOZZLE
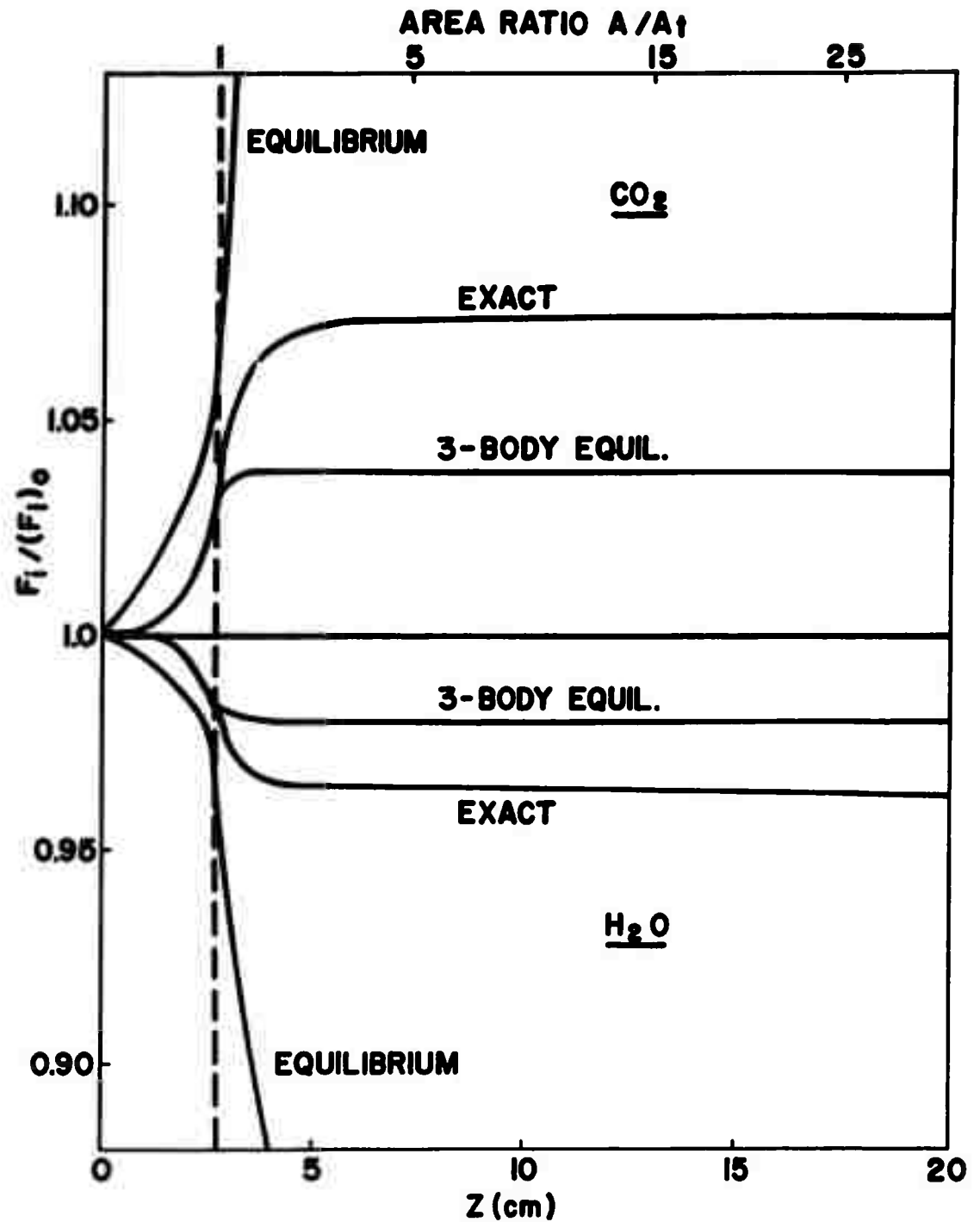
Ordinate Expressed as Fraction of Inlet Concentration

Fig. IV-4 CALCULATED SPECIES CONCENTRATIONS VERSUS DISTANCE
IN A 25° TOTAL ANGLE NOZZLE

Ordinate Expressed as Fraction of Inlet Concentration

the temperature is concerned, is practically indistinguishable from frozen flow. The 3-body equilibrium solution is even closer to the frozen flow limit. The same thing is shown in Fig. IV-2 for the static pressure profile except that the differences are even less marked - a well-known fact which should emphasize the great difficulty of deducing anything reliable about the chemical kinetics of nozzle flow from pressure measurements alone.

Figs. IV-3 and IV-4 show the variations in the four major reactive species expressed as fractions of the inlet concentrations (F_i is the number of moles of species i per unit mass of mixture). These bring out much more strikingly the great deviation of the exact calculation from the equilibrium flow limit. In the latter approximation the composition continues to shift drastically all the way down the nozzle as the temperature and pressure decrease (only a small part of this shifting equilibrium could be conveniently included in the scale of the graphs). In the actual exact chemical kinetic case, however, the composition changes less strongly at first and then rather abruptly "freezes" for all practical purposes in the region between $z \cong 4\text{-}6$ cm. This is the type of behavior first noted by Bray (Ref. 3) in an analytical study of a single recombination-dissociation reaction in nozzle flow. In the present case it is not the recombination reactions which freeze, however, but the main 2-body reactions $CO + OH \longrightarrow CO_2 + H$ and $H + H_2O \longrightarrow H_2 + OH$ since the exact calculation shows that the radical concentrations are still dropping sharply out to $z = 18$ cm or so. It should be possible to apply the Bray criterion for locating the approximate freezing point. This is

done by finding the point at which one of the derivatives, say dF_{CO}/dz, determined from the equilibrium solution becomes equal to the reverse rate term obtained from $H+CO_2 \longrightarrow CO+OH$, also using equilibrium concentrations. This procedure yielded a freezing point at about $z = 3$ cm, which is in fair agreement with that found from the exact calculation. A reasonable approximation to the flow could then be constructed by an equilibrium calculation down to the freezing point and a frozen calculation beyond.

The 3-body equilibrium solution is fairly close to the exact solution in Figs. IV-3 and IV-4, although it always indicates somewhat too small an extent of reaction. Use of this approximation is considerably simpler from the computation standpoint, since as shown previously (Ref. 1) the whole problem reduces to one rate equation in this case. It should be noted that the opposite approximation of assuming the 2-body reactions to be in equilibrium is really essentially equivalent to the assumption of complete equilibrium, since then the water gas equilibrium is maintained and this is the main one in the complete equilibrium solution. Thus, the fact that the exact solution deviates so markedly from this indicates that it is the 3-body rather than the 2-body reactions which are closer to equilibrium throughout. This may at first seem surprising until it is recalled that the 2-body reaction rates decrease exponentially with decreasing temperature while the 3-body rates increase somewhat, which must be sufficient to overcome the greater slowing effect of decreasing pressure on the 3-body rates.

An example of the effect of expansion angle on the gas composition is given in Fig. IV-5. Results with the exact calculation for CO and H_2 as a function of area ratio are shown for 25° and 12.5° nozzles. The expected influence of longer residence time in reaching a given area for the 12.5° nozzle is clearly shown, as at any area ratio a greater change in concentration has occurred. This is reflected in higher temperature, of course, and to a lesser extent in higher gas velocity (specific impulse). In this example the difference between the results for the two nozzles is very small - about 1% higher exit velocity (for a pressure of 1 atm) in the 12.5° nozzle than the 25° nozzle.

References

1. Task R Quarterly Progress Report No. 9. APL/JHU Report TG 331-9.

2. W. G. Vincenti, AEDC-TN-61-65, Stanford Univ., May (1961).
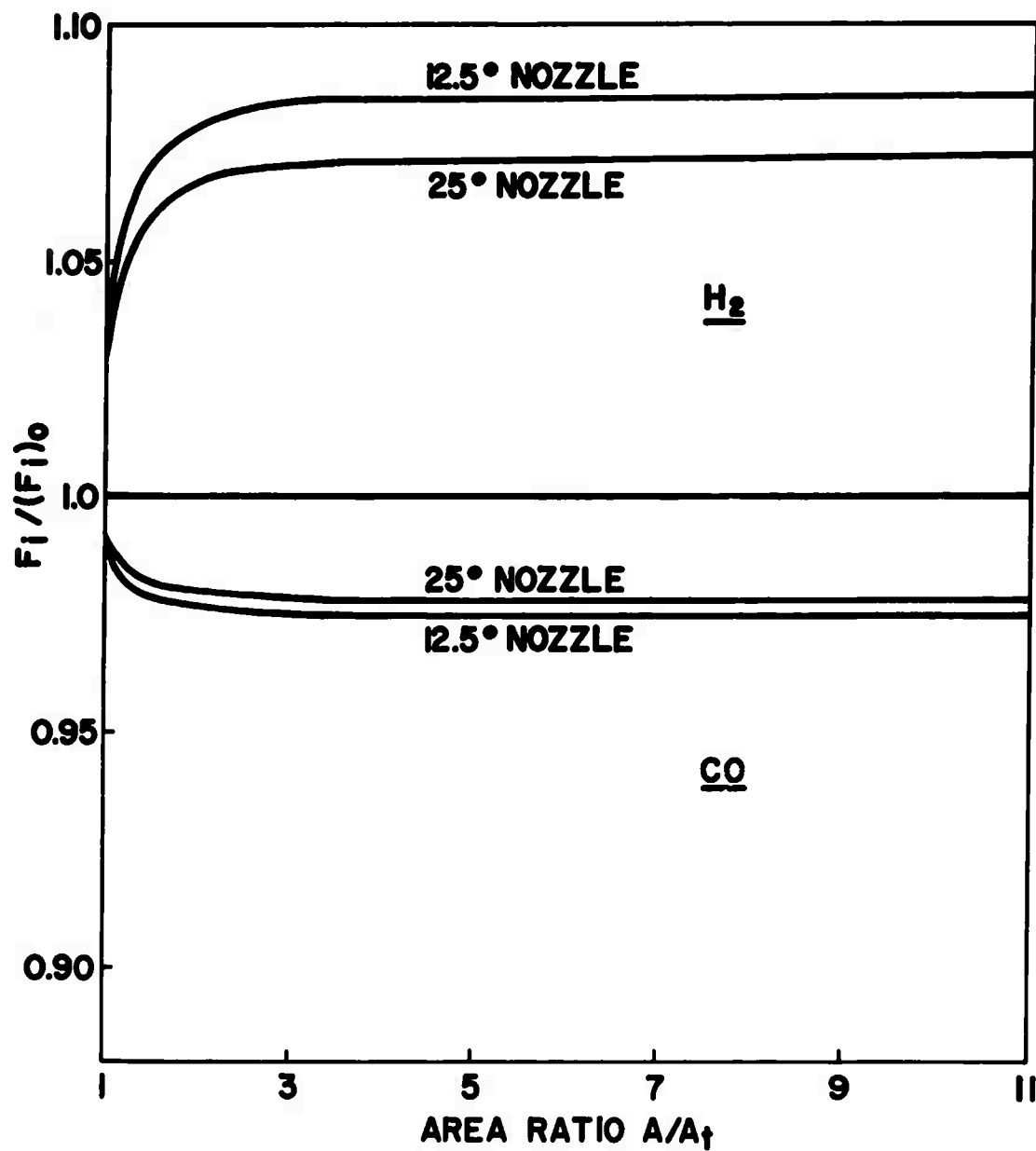
3. K. N. C. Bray, J. Fluid Mech. 6, 1 (1959).

Fig. IV-5 COMPARISON OF CALCULATED SPECIES CONCENTRATIONS VERSUS
AREA RATIO IN NOZZLES WITH DIFFERENT EXPANSION ANGLES

Ordinate Expressed as Fraction of Inlet Concentration

UNCLASSIFIED